Earth and Planetary Science Letters 284 (2009) 489–503

Contents lists available at ScienceDirect

Earth and Planetary Science Letters

journal homepage: www.elsevier.com/locate/epsl

Detrital-zircon geochronology of the eastern Magallanes foreland basin: Implications for Eocene kinematics of the northern Scotia Arc and Drake Passage

David L. Barbeau, Jr. [a,*], Eduardo B. Olivero [b], Nicholas L. Swanson-Hysell [a,1], Khandaker M. Zahid [a], Kendra E. Murray [a,2], George E. Gehrels [c]

[a] Department of Geological Sciences, University of South Carolina, 701 Sumter Street, EWS 617, Columbia, SC 29208, USA
[b] Centro Austral de Investigaciones Científicas, CADIC-CONICET, B. Houssay 200, 9410 Ushuaia, Tierra del Fuego, Argentina
[c] Arizona LaserChron Center, Department of Geosciences, University of Arizona, 1040 E. Fourth Street, Tucson, AZ 85721, USA

ARTICLE INFO

Article history:
Received 10 January 2009
Received in revised form 15 April 2009
Accepted 12 May 2009
Available online 4 July 2009

Editor: T.M. Harrison

Keywords:
provenance
Drake Passage
Antarctica
Andes
U/Pb geochronology

ABSTRACT

U/Pb detrital-zircon geochronology of eleven sandstones collected from Cretaceous through Oligocene strata of the eastern Magallanes foreland basin of southernmost Argentina records a dramatic provenance shift near the end of the middle Eocene at ca. 39 Ma. From the Late Cretaceous through most of the middle Eocene, detrital zircons reaching the foreland basin were dominantly contributed from ≤140 Ma sources, most likely derived from the Patagonian–Fuegian magmatic arc. In contrast, detrital-zircon populations of sampled upper Eocene and Oligocene strata are dominated by 150–190 Ma and pre-Mesozoic grains presumably derived from ignimbrites and granitoids associated with the break-up of Gondwana and from metasedimentary rocks of the Cordillera Darwin metamorphic complex, respectively. Exposures of these units occur in the hinterland of the Fuegian Andes thrust belt and inboard of the Patagonian–Fuegian batholith, suggesting that middle to late Eocene shortening in the rear of the Fuegian orogenic wedge structurally dammed batholith-derived sediment from reaching the foreland basin while contributing Jurassic and pre-Mesozoic detritus from hinterland thrust sheets. The timing of this interpreted deformation is in agreement with (1) independent structural, stratigraphic, and thermochronometric evidence of middle Paleogene deformation in the Fuegian Andes, and (2) marine Nd isotope ratio data that reveal initial penetration of Pacific water through the Drake Passage, thereby suggesting a possible link between the kinematics of the Fuegian Andes, the opening of Drake Passage, and if related, the Oi-1 glaciation of Antarctica.

© 2009 Elsevier B.V. All rights reserved.

1. Introduction

The Fuegian Andes currently form the southern terminus of the 8000 km long Andean mountain belt. However, as recently as the Paleogene this subduction-related orogen continued at least 1000 km farther south by connection with the Antarctic Peninsula (Dalziel and Elliot, 1971). The progressive Cenozoic dismemberment of this mountain belt formed the Scotia Arc, an assemblage of continental and transitional crust occupying the southwestern part of the Southern Ocean's Atlantic sector (Fig. 1A). The development of the Scotia Arc is associated with the opening of Drake Passage between the Antarctic (ANT) and South American (SAM) plates, thereby forming the Scotia (SCO) and associated microplates and resulting in significant changes to global ocean circulation. A prominent hypothesis for the earliest Oligocene (Oi-1) glaciation of Antarctica (Miller et al., 1991; Zachos et al., 2001) posits that the opening of this marine gateway removed the final continental barrier to the development of the Antarctic circumpolar current (ACC), which now thermally isolates Antarctica from warm ocean gyres, and allowed for the development of persistent large ice sheets (Barker and Burrell, 1977; Kennett, 1977).

Although recent numerical modeling favors the Paleogene drawdown of atmospheric CO_2 (Pagani et al., 2005) and albedo feedback as the primary drivers of middle Cenozoic glaciation of Antarctica (DeConto and Pollard, 2003; Huber and Nof, 2006), the role of the ACC in Paleogene ice-volume increase and global cooling is widely debated, largely because the timing of Drake Passage opening and onset of the ACC remains contentious. Currently, the oldest known oceanic crust in the Scotia Sea dates to the late Oligocene (Barker and Burrell, 1977; Eagles et al., 2005), which Barker (2001) employed to interpret an early Miocene onset of the ACC. Pelagic stratigraphic architectures in the Southern Ocean have been interpreted to indicate a late Oligocene onset of the ACC (Pfuhl and McCave, 2005; Lyle et al., 2007; Koenitz et al., 2008). If correct, these interpretations preclude an ocean circulation mechanism for the Oi-1 glaciation of Antarctica.

* Corresponding author.
E-mail addresses: dbarbeau@geol.sc.edu (D.L. Barbeau), emolivero@gmail.com (E.B. Olivero), ggehrels@geo.arizona.edu (G.E. Gehrels).
[1] Present address: Department of Geosciences, Princeton University, Princeton, NJ, 08544, USA.
[2] Present address: Department of Geosciences, University of Arizona, Tucson, AZ, 85721, USA.

0012-821X/$ – see front matter © 2009 Elsevier B.V. All rights reserved.
doi:10.1016/j.epsl.2009.05.014

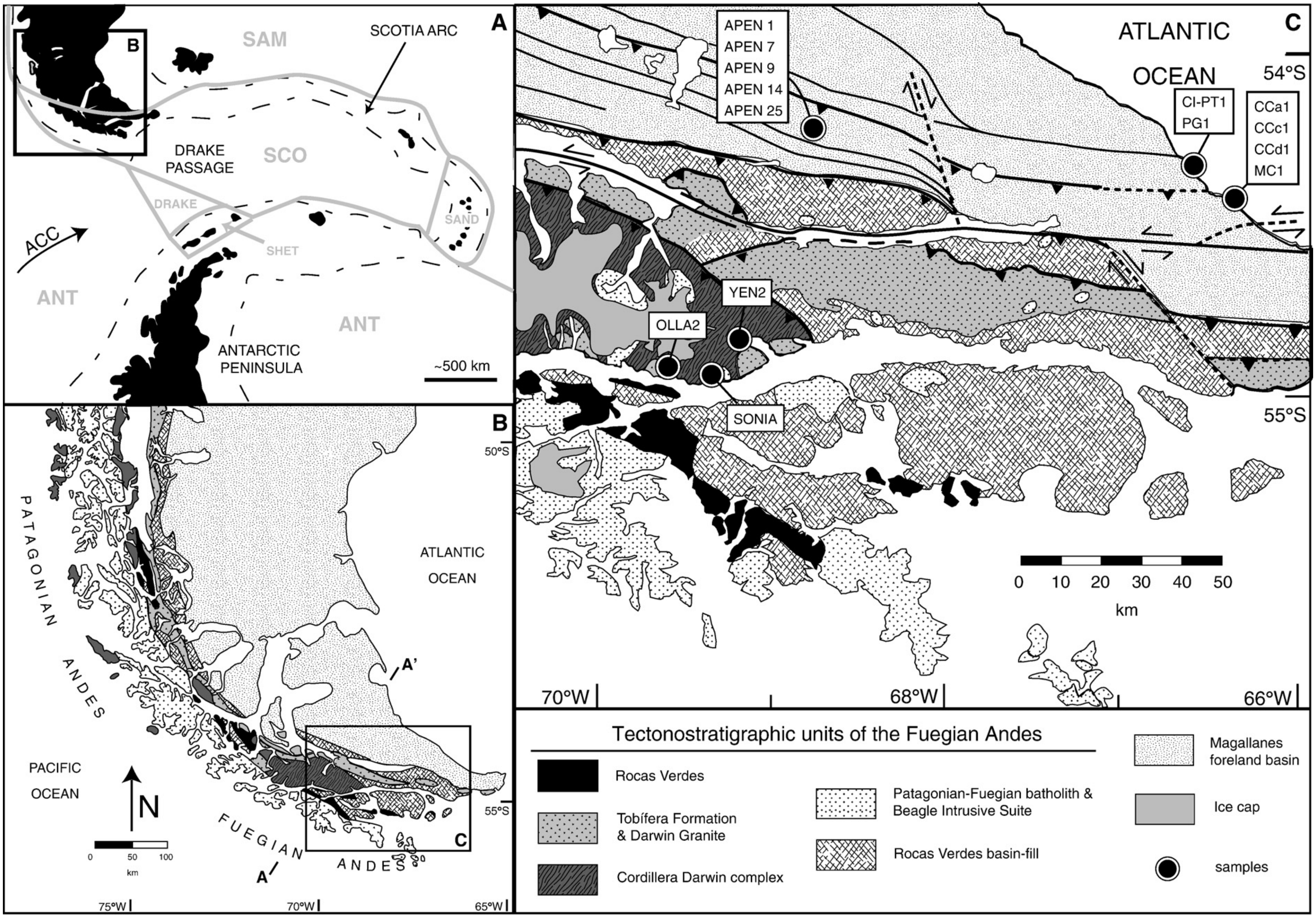

Fig. 1. Maps of the study area. A. Scotia Arc including the southernmost Andes, Antarctic Peninsula and sub-Antarctic islands. The Antarctic Circumpolar Current (ACC) connects the Pacific and Atlantic sectors of the Southern Ocean through Drake Passage and thermally isolates Antarctica from warm pole-ward ocean currents. Tectonic plates and plate boundaries are shown in gray: ANT: Antarctica, SCO: Scotia, SAM: South America, SHET: South Shetland, SAND: South Sandwich. B. Simplified geology of southernmost South America and Tierra del Fuego. Geologic patterns as in C. Location of cross-sections in Fig. 5 depicted by line A–A'. C. Simplified geologic map of study area showing location of samples. Geology compiled and modified from Wilson (1991), Klepeis (1994a,b), Kohn et al. (1995), Fildani and Hessler (2005), Olivero and Malumián (2008), and fieldwork conducted by the first three authors.

In contrast to interpretations of latest Paleogene or early Neogene development of the ACC, several lines of evidence point towards a zenith of plate tectonic activity in the Scotia Arc and Drake Passage preceding the Oi-1 glaciation: (1) water-mass provenance data from the Atlantic sector of the Southern Ocean are consistent with late middle Eocene penetration of Pacific water through Drake Passage (Scher and Martin, 2006); (2) the accumulation of lower Eocene strata in southernmost South America has been interpreted as evidence of coeval crustal thinning (Ghiglione et al., 2008); and (3) thermochronometric data from the Fuegian Andes of the northern Scotia Arc suggest rapid tectonic exhumation from 60–30 Ma (Nelson, 1982; Kohn et al., 1995; Mukasa and Dalziel, 1996; Gombosi et al., 2009).

As the dominant western component of the northern limb of the Scotia Arc (Fig. 1), the Fuegian Andes should preserve an important record of the region's kinematic history. Sandbox models have been used to suggest that the curvature of the Patagonian and Fuegian Andes may date to the Cretaceous (Diraison et al., 2000; Ghiglione and Cristallini, 2007). However, the Fuegian Andes display several characteristics that indicate greater Late Cretaceous–Paleogene contractional deformation than in their Patagonian counterpart to the northwest, including: (1) exhumed amphibolite-facies hinterland rocks (Klepeis, 1994a; Kohn et al., 1995), (2) significantly larger shortening estimates (Kraemer, 2003), (3) greater and faster Paleogene foredeep subsidence (Biddle et al., 1986) and (4) significant contraction in the Magallanes basin fold–thrust belt during the Eocene (Torres Carbonell et al., 2008). These observations are consistent with progressive anticlockwise vertical-axis rotation (oroclinal bending) of the Fuegian Andes, which would have had a profound effect upon the opening of Drake Passage via rotation-induced separation between the Antarctic Peninsula and the southernmost Andes. Regional kinematic analysis of the southern Andes should evaluate this hypothesis, and provide insight into the timing and magnitude of displacements in the Scotia Sea. In this paper, we contribute new sediment composition data that record a dramatic provenance shift adjacent to the Fuegian Andes in the eastern Magallanes foreland basin that is coeval with other evidence for the opening of Drake Passage.

Sedimentary provenance analysis can constrain the sources and transport pathways of detrital sediments. As a result, foreland basin sediment provenance data have provided important constraints on the reconstruction of the kinematic history of mountain belts (e.g., DeCelles et al., 1993; Robinson et al., 2001; Horton et al., 2002; Najman et al., 2005). Here, we examine the exhumational history of the Fuegian Andes through the lens of sediment provenance of the adjacent Magallanes foreland basin in order to better determine the kinematic history of the orogen. We report ~1200 single-grain detrital-zircon U/Pb ages collected from eleven Cretaceous and Paleogene sandstones and a single pre-Jurassic metasedimentary sample analyzed by laser-ablation inductively coupled plasma multi-collector mass-spectrometry (LA-MC-ICP-MS). To aid in the interpretation of our results, we also report the U/Pb crystallization ages of two felsic orthogneisses from the Cordillera Darwin complex. Because of its refractory nature, high concentration of radiogenic U (10 ppm–1 wt.%), abundance within the continental crust, and durability in the supracrustal environment, zircon has proven to be a particularly useful tool for modern sedimentary provenance analysis. In addition to improving depositional age constraints from unfossiliferous and/or poorly magnetized strata (Fildani et al., 2003; DeCelles et al., 2007), U/Pb detrital-zircon geochronology can be valuable for fingerprinting tectonostratigraphic units (e.g., Weislogel et al., 2006).

2. Geologic setting

The Cretaceous–Cenozoic Magallanes foreland basin system accumulated a near-complete detrital stratigraphy associated with the orogenic development of the Patagonian and Fuegian Andes (Olivero and Malumián, 2008 and references therein). Hence, its contents comprise a valuable compositional and kinematic record of the southern terminus of this important mountain belt. Fig. 1 and the following sub-sections provide a brief overview of the history and tectonostratigraphy of the orogen.

2.1. Geologic history

The southern Andes formed along the western margin of South America during Late Jurassic to Recent subduction of Pacific oceanic lithosphere, contemporaneous with and related to the progressive opening of the south Atlantic Ocean basin. This tectonic history began coevally with the voluminous eruption of Jurassic rhyolitic and silicic ignimbrites and emplacement of felsic plutons that formed a silicic large igneous province recognized in Patagonia and West Antarctica (Pankhurst et al., 1998) with mafic intrusions also known in the Karoo province of South Africa (Pankhurst et al., 2000), all of which have been tied to the initial break-up of Gondwana (Riley and Leat, 1999; Pankhurst et al., 2000). South America's resultant westward migration relative to Africa instigated contractional tectonics along its leading edge. This contraction resulted in east-dipping subduction and associated calc-alkaline magmatism starting in the latest Jurassic that continues north of the SCO–SAM–ANT triple junction today (Hervé et al., 2007).

The initial Late Jurassic–Early Cretaceous subduction system coincided with the development of the ocean-margin Rocas Verdes sedimentary basin inboard of the nascent magmatic arc (Dalziel et al., 1974) in which a thick succession of volcaniclastic and other detrital sedimentary rocks were deposited (Wilson, 1991; Olivero and Martinioni, 2001; Willan and Hunter, 2005; Fildani and Hessler, 2005; Olivero and Malumián, 2008). Retro-arc contractional deformation in the southern Andes began soon after deposition of the Rocas Verdes succession, resulting in: (1) its inversion and shortening (Wilson, 1991; Fildani et al., 2003); (2) obduction of its basin-floor pseudo-ophiolitic rocks (Wilson, 1991); and (3) locally deep burial of the aforementioned Gondwana break-up volcanics (Galáz et al., 2005) and underlying accretionary prism rocks formed during the Paleozoic–early Mesozoic Gondwanide orogeny (Kohn et al., 1995; Faundez et al., 2002; Thomson and Herve, 2002; Hervé et al., 2003).

Continued shortening through the end of the Paleogene (1) loaded the southern South American crust causing flexural subsidence and accumulation of a thick succession of dominantly marine detrital strata in the Magallanes foreland basin (Biddle et al., 1986; Wilson, 1991; Olivero and Malumián, 1999, 2008); (2) exhumed metasedimentary, volcanic and plutonic rocks of the Fuegian Andes hinterland, including the Cordillera Darwin complex (Nelson, 1982; Kohn et al., 1995; Mukasa and Dalziel, 1996); and (3) caused thin-skinned deformation across the proximal Magallanes foreland basin to form the Magallanes thrust belt (Wilson, 1991; Klepeis, 1994a; Fildani et al., 2003; Kraemer, 2003; Fildani and Hessler, 2005; Ghiglione and Ramos, 2005; Olivero and Malumián, 2008; Torres Carbonell et al., 2008). Beginning in the latest Oligocene or early Neogene, convergence in the southernmost Andes decreased dramatically, coincident with the origin of the SCO–SAM sinistral transform boundary that remains active today (Fig. 1; Klepeis, 1994b; Ghiglione and Ramos, 2005).

2.2. Tectonostratigraphy & candidate zircon sources

The Fuegian Andes are composed of five main tectonostratigraphic units (Fig. 1C). Variations in the zircon composition of these units, described below and in Fig. 2, allow the exhumational history of the orogen to be reconstructed via detrital-zircon provenance of eastern Magallanes foreland basin sediments.

2.2.1. Southern Andean metamorphic complexes

The Cordillera Darwin complex is a large, polydeformed assemblage of pelitic and metavolcanic phyllites, schists and gneisses that resides in the core of the Fuegian Andes with an average elevation

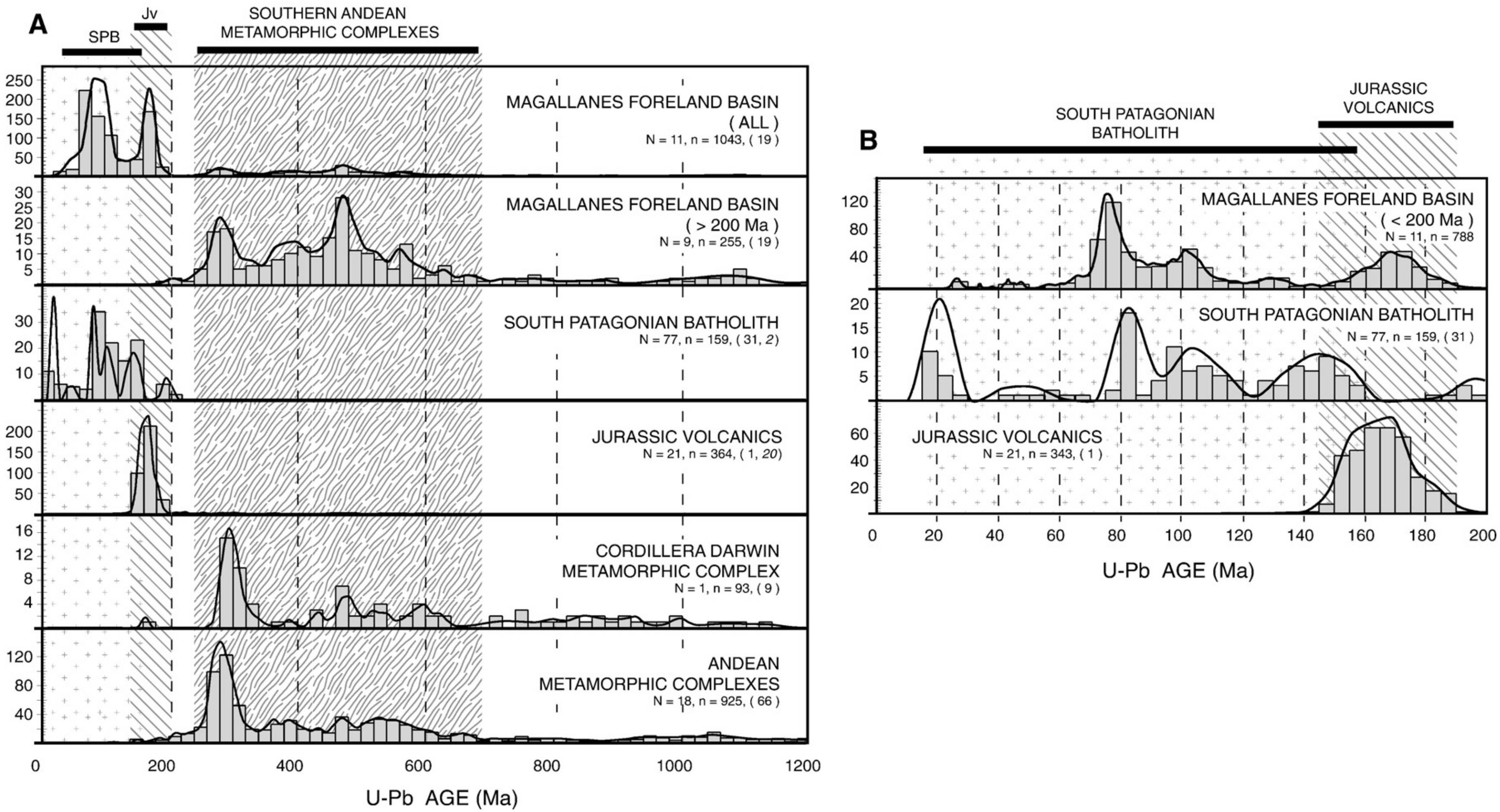

Fig. 2. Composite histograms and probability plots of the crystallization ages of relevant tectonostratigraphic units from study area and equivalent units in Patagonia and the Antarctic Peninsula. A. Distribution of all detrital-zircon U/Pb ages collected from Cretaceous–Oligocene sandstones of the eastern Magallanes foreland basin (this study) compared to crystallization ages reported from the South Patagonian–Fuegian batholith (Hervé et al., 2007); Jurassic volcanic rocks occurring in southern South America and the Antarctic Peninsula associated with the break-up of Gondwana (Féraud et al., 1999; Pankhurst et al., 2000); detrital-zircon U/Pb ages collected from a metasedimentary sample (SONIA1) of the Cordillera Darwin complex (this study); and detrital-zircon U/Pb ages collected from metasedimentary complexes in the Patagonian Andes (Hervé et al., 2003). B. Close-up of post-Triassic age distributions of Magallanes foreland basin detrital zircons (this study), the South Patagonian–Fuegian Batholith (Rolando et al., 2002; Hervé et al., 2007) and the Jurassic volcanic rocks associated with the break-up of Gondwana. In both figures, the patterned polygons depict the dominant age populations of each candidate source for comparison to the foreland basin detrital-zircon age distributions that are the focus of this study. The numbers in parentheses following numbers of samples (*N*) and analyzed grains (*n*) indicate the numbers of grains that plot outside of the plotted range of ages (plain font) and within the plotted range but lacking sufficiently concentrated age populations to be visible (italicized font). See Supplementary material for all data and metadata.

more than 1000 m greater than the surrounding stratigraphy. Although similar to other pre-Jurassic metamorphic complexes of the southern Andes (Hervé and Fanning, 2003; Hervé et al., 2003; Augustsson et al., 2006), it is distinguished by garnet- to sillimanite-bearing amphibolite facies, which record peak temperatures and pressures exceeding 650 °C and 10 kbar (Kohn et al., 1995). Integration of these thermobarometric estimates with $^{40}Ar/^{39}Ar$ and fission-track thermochronology indicate that this hinterland complex was exhumed from depths as great as 30 km between 90–70 and 60–40 Ma (Nelson, 1982; Kohn et al., 1995). The mechanism of exhumation has been widely debated between thick-skinned uplift, antiformal stack, and metamorphic core complex interpretations (e.g., Dalziel and Brown, 1989; Klepeis, 1994a; Kohn et al., 1995; Kraemer, 2003).

Although detrital-zircon data from the Cordillera Darwin metamorphic complex have not been reported prior to this study, the zircon composition of the metamorphic complexes of the Patagonian Andes is well-documented (Fig. 2A), with a large well-defined 250–350 Ma population likely derived from the Gondwanide belt formed during the Carboniferous–Permian assembly of Patagonia and its amalgamation to mainland South America (Hervé and Fanning, 2003; Hervé et al., 2003; Augustsson et al., 2006). Many of the southern Andean metamorphic complexes also contain significant but broadly dispersed 400–700 Ma populations, presumably derived from rocks associated with the Famatinian and Pampean belts prevalent in central South America (ibid.). Samples from the eastern Andean metamorphic complex, which resides in a similar inboard position as the Cordillera Darwin complex, also contain significant 900–1200 Ma zircons (Hervé et al., 2003), likely derived from adjacent regions in the central Andes, southern Africa and perhaps East Antarctica.

2.2.2. Gondwana dispersal volcanic rocks and granitoids

The Tobífera/Lemaire Formations and Darwin intrusive suite are the southern South American components of the aforementioned silicic ignimbrites, volcaniclastic rocks and felsic plutons associated with Jurassic break-up of Gondwana (Riley and Leat, 1999; Pankhurst et al., 2000). Whereas the current exposure of the Darwin suite is largely confined to Cordillera Darwin, the volcanogenic Tobífera/Lemaire Formations are widely exposed in the Fuegian Andes hinterland thrust sheets (Fig. 1), including those of Cordillera Darwin, but also occur widely in the subsurface and foreland massifs throughout much of southernmost South America where they underlie Cretaceous and younger strata (Biddle et al., 1986; Wilson, 1991; Pankhurst et al., 2000). Although reported U/Pb zircon ages from the Tobífera/Lemaire Formations and Darwin suite are relatively rare (Mukasa and Dalziel, 1996; Pankhurst et al., 2000), genetically related and compositionally similar strata throughout southern South America and the Antarctic Peninsula are well dated (Pankhurst et al., 2000). With a distribution of crystallization ages spanning ca. 145–190 Ma and centered upon 170 Ma (Fig. 2; Féraud et al., 1999; Pankhurst et al., 2000), these rocks compose the only prominent primary source of Jurassic zircons in the regions surrounding the study area. In the adjacent Patagonian Andes, thermobarometry estimates of 6 kbar and 400 °C indicate that Andean mountain-building exhumed these rocks from depths of 20–25 km (Galáz et al., 2005).

2.2.3. Rocas Verdes basin

The Rocas Verdes *sensu stricto* are a complex of gabbros, sheeted dikes, pillow basalts and tonalites that are interpreted as having formed the floor of the middle Mesozoic Rocas Verdes marginal basin (Stern et al., 1992; Cunningham, 1994), inboard of the Patagonian–Fuegian magmatic arc (Fig. 1B & C). Given its predominantly mafic composition, the Rocas Verdes complex is an improbable source of detrital zircons, although zircon separates from rare, cogenetic tonalites of the Sarmiento complex have yielded 140–150 Ma U/Pb ages (Stern et al., 1992).

The Yahgan, Beauvoir, Zapata and La Paciencia Formations comprise a thick succession of Late Jurassic and Cretaceous marine volcaniclastic and siliciclastic strata that formed the Rocas Verdes basin-fill (Dalziel and Elliot, 1971; Olivero and Martinioni, 2001; Olivero and Malumián, 2008), which has been greatly shortened and metamorphosed to greenschist facies (Cunningham, 1994; Kraemer, 2003). The fine caliber of most of the Rocas Verdes basin-fill precludes it from being a significant source of zircons for the subsequent Magallanes foreland basin. The sandstones present in the basin-fill were deposited close to the magmatic arc and contain andesitic lithic fragments (Olivero, 2002). The presence of such lithic fragments suggests that, if present, Rocas Verdes basin-fill detrital zircons were derived from the coeval Patagonian–Fuegian magmatic arc.

2.2.4. Patagonian–Fuegian magmatic arc

The Patagonian–Fuegian batholith is a calc-alkaline igneous suite dominated by tonalites with subordinate granites and gabbros (Rolando et al., 2002; Hervé et al., 2007). From the Late Jurassic to the Neogene (Hervé et al., 2007), this magmatic arc contributed voluminous crustal material to the western margin of southernmost South America (Fig. 1B & C) where it intruded country rock largely composed of the relict Gondwanide accretionary prism (Hervé et al., 2003). A compilation of U/Pb zircon ages determined from the Patagonian sector (Rolando et al., 2002; Hervé et al., 2007) provides a proxy record of this protracted felsic magmatism, and highlights apparent pulses of activity centered at 150, 105 and 85 Ma (Fig. 2). In addition to the cohesive Patagonian–Fuegian batholith, cogenetic arc-related intrusive rocks occur further inboard in the Cordillera Darwin and Rocas Verdes thrust sheets of the Fuegian Andes where they are locally known as the Beagle intrusive suite (Kohn et al., 1995).

2.2.5. Magallanes foreland basin and thrust belt

From the Late Cretaceous through the Paleogene, flexural subsidence inboard of the Fuegian and Patagonian Andes accumulated a thick succession of strata in submarine-fan, shelf, shallow-marine and deltaic settings, forming the Magallanes foreland basin (Fig. 1B & C; Biddle et al., 1986; Olivero and Malumián, 1999; Fildani et al., 2003; Fildani and Hessler, 2005; Ghiglione and Ramos, 2005; Olivero and Malumián, 2008; Torres Carbonell et al., 2008). Integration of sediment transport directions from throughout the basin (Winn and Dott, 1979; Dott et al., 1982; Macellari et al., 1989; Martinioni et al., 1999; Olivero et al., 2003; Olivero and Malumián, 2008) indicate that sediment in the eastern Magallanes basin was transported directly from the adjacent mountain belt.[3] This orogen-perpendicular transport is also indicated by sediment petrography constraints on provenance (Olivero, 2002) and across-axis progradation directions depicted in seismic sections (Biddle et al., 1986; Galeazzi, 1998).

Broadly synchronous northward migration of the Fuegian orogenic wedge progressively entrained these strata into the thin-skinned Magallanes foreland thrust belt (Klepeis, 1994a; Ghiglione and Ramos, 2005; Olivero and Malumián, 2008; Torres Carbonell et al., 2008) that comprises the frontal part of the Fuegian orogen (Fig. 1B & C).

Detrital zircons recovered from Upper Cretaceous strata of the northern/western Magallanes foreland basin are dominated by a large 90–150 Ma population, with subordinate, poorly defined populations with U/Pb ages scattered between the Mesoproterozoic and the Early Jurassic (Fildani et al., 2003; Romans et al., in press). Heretofore,

[3] See Appendix S1 for detailed discussion of sediment transport directions in the greater Magallanes basin.

detrital-zircon U/Pb ages have not been published from Argentine Tierra del Fuego, or from Paleogene strata anywhere in the Magallanes foreland basin.

3. Sampled stratigraphy

The sampled units include a single quartzite sample and two felsic/silicic orthogneisses collected from the southern margin of the Cordillera Darwin complex, and eleven sandstones collected from the Argentine sector of the Magallanes foreland basin (Fig. 1C). In addition to brief descriptions below, more detailed contextual information is presented in Appendix S2 and Table S1 of the online supplementary materials, including sample descriptions and locations, and depositional age constraints.

3.1. Crystalline rocks of the Fuegian Andes' orogen

Sample SONIA1 was collected from a quartz-schist that occurs locally at Caleta Sonia along the northern shore of the Beagle Channel in Chilean Tierra del Fuego. The sampled interval constitutes part of the comparatively low-grade rocks of the Cordillera Darwin complex that occur between Bahia Yendegaia and Punta Yamana along the Beagle Channel (Kohn et al., 1995). Our additional sampling of Cordillera Darwin metamorphic rocks did not produce detrital zircons, but instead has revealed new occurrences of felsic to silicic orthogneisses: Samples OLLA2 and YENDEGAIA2 were collected from fine- to medium-grained, well-bedded gneissic strata exposed in the southeastern Cordillera Darwin at Caleta Olla and Bahia Yendegaia, respectively.

3.2. Magallanes foreland basin strata

Upper Cretaceous samples APEN14 and APEN7 and Paleocene samples APEN25 and APEN1 were collected from litharenitic strata in the Sierra de Apen of central Tierra del Fuego. Lower Eocene sample CI-PT1 was collected from a thick succession of dark gray mudstones and subordinate sandstones in the Punta Torcida Formation that occurs north of Cabo Irigoyen of the Atlantic coast. Middle Eocene sample APEN9 comes from a thin litharenite associated with a polymict pebble–cobble conglomerate, collected from the foothills of Sierra de Apen. Upper Eocene samples CCa1, CCc1 and CCd1 of the Cerro Colorado Formation were collected from litharenites that occur east of Cerro Colorado along the Atlantic coast of Tierra del Fuego. Lower Oligocene sample MC1 is a coarse-grained to granular sublitharenite that occurs approximately 50 meters up-section from sample CCd1 in the same region. Oligocene sample PG1 is from a litharenite near Punta Gruesa along the Atlantic coast.

4. Methods

The collection, preparation and analysis of detrital-zircon samples largely follow the methods of Gehrels et al. (2006), with minor modifications described below. Sample preparation and documentation was performed at the Tectonics & Sedimentation Laboratory at the University of South Carolina. U/Pb zircon geochronology was performed at the Arizona LaserChron Center at the University of Arizona.

4.1. Sample collection and preparation

For each sample, approximately 5–10 kg of rock was collected from outcrops lacking evidence of large-scale soft-sediment deformation or other possible contaminants. Collected samples were disaggregated with a Bico WD Chipmunk jaw crusher, a Bico UD pulverizer, and a custom-built steel mortar and pestle. High-density minerals were initially concentrated with a MD Mineral Technologies MK 2 Gemeni table and hand-operated ABS plastic gold pans. Secondary heavy mineral concentration was completed with the heavy liquids sodium polytungstate (specific gravity of 2.89), LST (a lithium heteropolytungstate solution with specific gravity of 2.90) and/or methylene iodide (specific gravity of 3.30) in 125 mL Pyrex separatory funnels and/or 10 mL centrifuge tubes. Resulting heavy fractions were processed step-wise via 0.25 A increments (from 0.25 to 1.75 A) using a S.G. Frantz L1 isodynamic magnetic separator operating at horizontal and vertical angles of 15° and 25°, respectively. To eliminate possible biases associated with hand-picking, the resulting zircon-rich separates were poured into Buehler ring forms along with chips of a known zircon standard and NBS 610 trace element glass and bonded in place using double-sided tape and epoxy resin. The resulting mounts were gently polished using wet sandpaper of 2500 and 3000 grit in order to expose the grain cores.

4.2. U/Pb geochronology using LA-MC-ICP-MS

U/Pb detrital-zircon geochronology was conducted by LA-MC-ICP-MS in two sample runs conducted during April 2006 and May 2008. Analysis utilized grain ablation with a DUV193 ArF exciplex laser using spot diameters of 20–50 μm. The ablated material was carried in He gas into the plasma source of a GVI Isoprobe, which is equipped with a flight tube of sufficient width that U, Th, and Pb isotopes are measured simultaneously. All measurements were made in static mode, using 10^{11} Ω Faraday detectors for ^{238}U, ^{232}Th, ^{208}Pb, and ^{206}Pb, a 10^{12} Ω Faraday collector for ^{207}Pb, and an ion-counting channel for ^{204}Pb. Ion yields were ~1.0 mV per ppm. Each analysis consisted of one 20-second integration with the laser off, 20 one-second integrations with the laser firing, and a 30 s delay to purge for the next analysis. Each resulting ablation pit is ~15 μm in depth. For each analysis, measurement errors typically resulted in ~1–2% (2σ) age uncertainty. Common Pb correction was accomplished by using the measured ^{204}Pb and assuming an initial Pb composition from Stacey and Kramers (1975) with uncertainties of 1.0 for ^{206}Pb/^{204}Pb and 0.3 for ^{207}Pb/^{204}Pb. Our measurement of ^{204}Pb is unaffected by the presence of ^{204}Hg because backgrounds are measured on peaks (thereby subtracting any background ^{204}Hg and ^{204}Pb). Inter-element fractionation of Pb/U is generally ~20%, whereas fractionation of Pb isotopes is generally ~2%. In-run analysis of fragments of a large Sri Lankan zircon standard with known age of 564 ± 4 Ma (2σ) was used to correct for these fractionations. Interpreted ages are based on ^{206}Pb/^{238}U for < 1.0 Ga grains and on ^{206}Pb/^{207}Pb for > 1.0 Ga grains. Analyses that were > 30% discordant or > 5% reverse discordant were excluded from interpretations.

4.3. Determination of maximum depositional ages from detrital-zircon data

In strata lacking volcanogenic interbeds, radioactive diagenetic minerals, and/or microfossils sufficient for high-resolution biostratigraphy, detrital-mineral ages can provide valuable insight into maximum depositional ages (Fildani et al., 2003; DeCelles et al., 2007). However, there is a lack of consensus in the scientific community about the methods of constraining maximum depositional ages with U/Pb detrital-zircon geochronology (e.g., Fedo et al., 2003; Andersen, 2005). In the Magallanes basin, the temporal overlap between the biostratigraphic ages of our sampled units (Appendix S2) and felsic magmatism in the adjacent Patagonian–Fuegian arc decreases the possibility of a significant lag between the youngest zircons in a sample and the time of that sample's deposition. However, since a uniform method of interpreting the youngest zircon ages in a sample has not been adopted by the scientific community, we present as many as four candidate maximum depositional ages for each sample (Fig. 3), and choose the best candidate through consideration of contextual data. Given a data set of ~100 analyses, Gehrels et al.

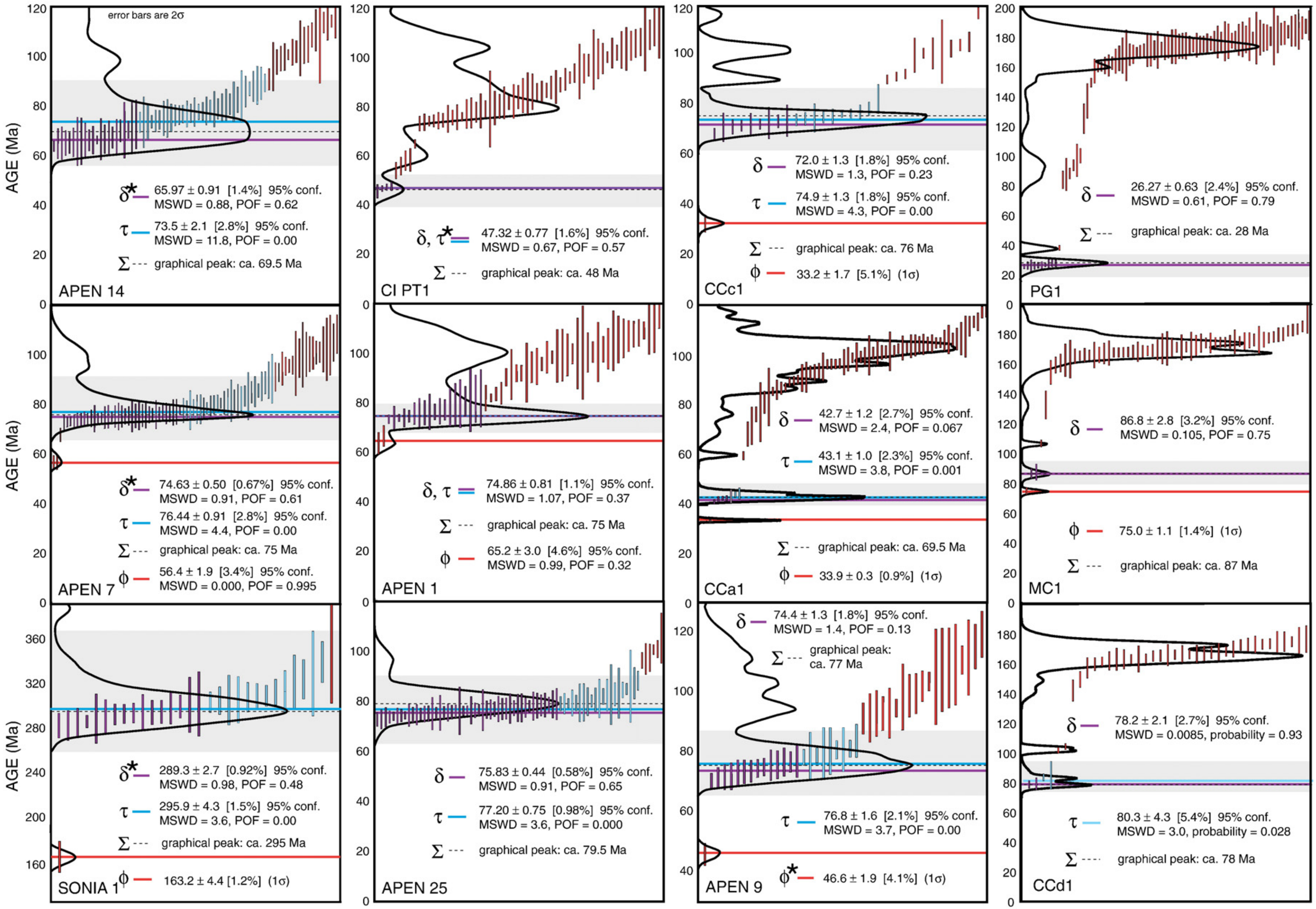

Fig. 3. Maximum depositional age interpretations from youngest detrital zircons analyzed from each sample. τ ages are the weighted mean age (as calculated using Ludwig, 1999) of all grains whose central values fall between the probability minima surrounding the youngest significant peak (defined as three or more grains that contain contributions to a single age-probability peak at the 2σ level). δ ages are the weighted mean age of all consecutively aged grains in the youngest significant peak whose 2σ errors overlap. Σ ages are the age of the graphical peak of the youngest significant population, which includes the portion of contributions to the peak at the 2σ level, regardless of whether the central age occurs within the peak. We also present the ages of younger peaks composed of less than three grains (ϕ ages). Age populations interpreted as depositional ages are marked with a superscript asterix (*).

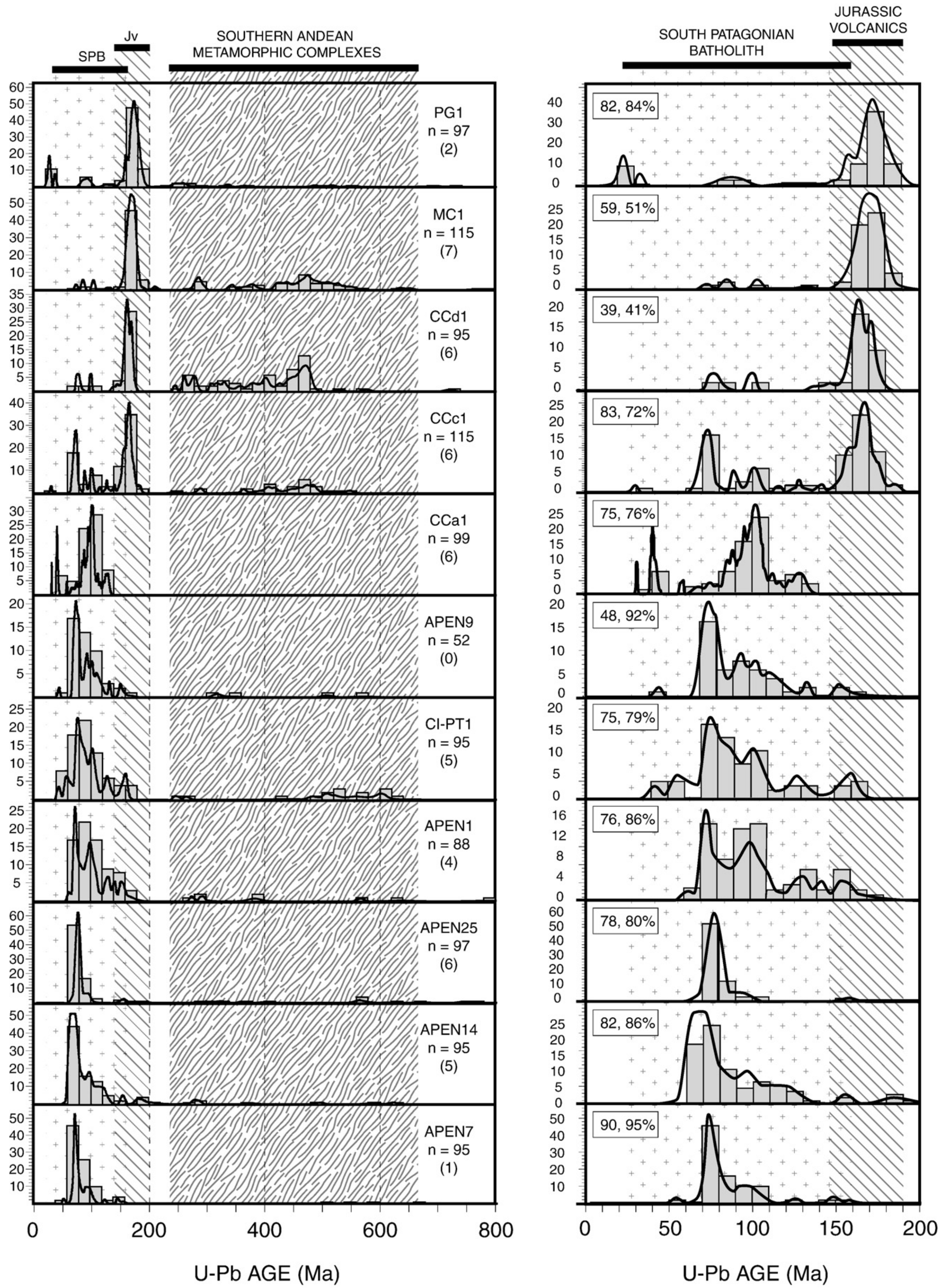
SPB
Jv
SOUTHERN ANDEAN
METAMORPHIC COMPLEXES
SOUTH PATAGONIAN
BATHOLITH
JURASSIC
VOLCANICS
PG1
n = 97
(2)
82, 84%
MC1
n = 115
(7)
59, 51%
CCd1
n = 95
(6)
39, 41%
CCc1
n = 115
(6)
83, 72%
CCa1
n = 99
(6)
75, 76%
APEN9
n = 52
(0)
48, 92%
CI-PT1
n = 95
(5)
75, 79%
APEN1
n = 88
(4)
76, 86%
APEN25
n = 97
(6)
78, 80%
APEN14
n = 95
(5)
82, 86%
APEN7
n = 95
(1)
90, 95%
U-Pb AGE (Ma)
U-Pb AGE (Ma)

(2006) define a significant population as three or more grains that contain contributions to a single age-probability peak at the 2σ level with the logic that it would be unlikely for three analyses that have been affected by Pb loss or inheritance to yield similar ages. Using that criterion, we report three maximum depositional age estimates for the youngest significant population in our age probability density distributions (Ludwig, 1999): (1) the mean age of all grains whose central values fall between the probability minima surrounding the youngest significant peak (τ ages); (2) the mean age of all consecutively aged grains in the youngest significant peak whose 2σ errors overlap (δ ages); and (3) the age of the graphical peak of the youngest significant population, which includes the portion of contributions to the peak at the 2σ level, regardless of whether the central age occurs within the peak (Σ ages). As demonstrated in Fig. 3, the adoption of δ ages yields significantly superior values for the mean square of weighted deviates (MSWD) and probability of fit (POF) in comparison to τ ages, thereby indicating a higher likelihood of the grains coming from a single age population. In addition to these age estimates for 'significant' peaks (*sensu* Gehrels et al., 2006), we also present the ages of younger peaks composed of less than three grains (ϕ ages).

5. Results

We present U/Pb detrital-zircon ages for the eleven sandstone samples collected from upper Cretaceous to Oligocene strata of the Magallanes foreland basin in Argentine Tierra del Fuego along with a single quartzite sample and two felsic/silicic orthogneisses from the southern margin of Cordillera Darwin. These results are depicted graphically as probability density distributions (Ludwig, 1999) in Figs. 2–5. Tabulated data (Table S2), and concordia & crystallization-age plots (Figs. S1 and S2) are presented in the online supplementary materials.

5.1. Maximum depositional ages

In Fig. 3, we show the youngest single-grain detrital-zircon ages recovered from each sample. Irrespective of the maximum depositional age criteria employed, our results warrant reconsideration and/or minor modification of the interpreted depositional ages of some of the studied units, although the zircon ages from most samples are consistent with biostratigraphically assigned ages.

The youngest significant age peak from the Cordillera Darwin complex sample SONIA1 spans 260–370 Ma, with τ, δ and Σ ages of 295.9 ± 4.3, 289.3 ± 2.7, and ca. 296 Ma, respectively. A one-grain ϕ age of 163 ± 8 Ma is significantly younger than the other estimates and biostratigraphic & detrital-zircon maximum depositional ages for broadly equivalent metasedimentary units in the Patagonian Andes (Hervé and Fanning, 2003; Hervé et al., 2003). The superior MSWD and POF values favor use of the δ age over the τ age for constraining maximum depositional age.

The age interpretations for the youngest significant detrital-zircon peak from upper Cretaceous sample APEN7 cluster around 75 Ma, although a ϕ two-grain age of 56.4 ± 1.9 Ma suggests that this sample may be younger. In light of MSWD and POF values and regional geologic relationships (see Appendix S2) we favor the 75 Ma interpretation, which is consistent with the biostratigraphic ages of the sampled unit's interpreted equivalents: the Policarpo (Maastrichtian–Danian) and Bahía Thetis Formations (late Campanian–early Maastrichtian). The youngest peak of detrital-zircon ages from the broadly equivalent sample APEN14 spans from ca. 60–80 Ma. Given the favorable MSWD and POF values and consideration of the biostratigraphy, we interpret the δ age of 65.97 ± 0.91 Ma as the maximum depositional age of sample APEN14.

The youngest significant detrital-zircon age peak in the Paleogene sample APEN25 ranges between ca. 73–88. Considering the comparable δ, τ and Σ ages constrained from this peak, we favor the δ age of 75.83 ± 0.44 Ma as a detrital-zircon maximum depositional age. These results are consistent with but significantly older than the late Paleocene palynology ages of ca. 55 reported by Martinioni and others (1999), which we use for our interpretations below. The youngest significant detrital zircon peak in sample APEN1 has δ, τ and Σ ages that roughly coincide at ca. 75 Ma, although a ϕ age of 65.2 ± 3.0 Ma suggests that this sample might be significantly younger. All of these maximum depositional ages are consistent with the unit's biostratigraphically assigned late Paleocene–early Eocene depositional age of ca. 53 Ma (Buatois and Camacho, 1993), which we use for our provenance and kinematic reconstructions. The δ and τ maximum depositional ages of 47.32 ± 0.77 Ma for sample CI-PT1 of the Punta Torcida Formation are identical and consistent with the Σ age, all of which are in conflict with the biostratigraphically determined middle early Eocene (50–52 Ma) age of the Punta Torcida Formation (Olivero and Malumián, 1999). As a result of the robust nature of the youngest significant detrital-zircon age peak, we utilize 47.3 Ma as the depositional age for the sampled unit.

The youngest significant peak from sample APEN9 spans ca. 71–82 Ma, which encompasses the Σ, τ and δ ages. However, we favor a maximum depositional age represented by a single 46.6 ± 3.8 Ma zircon that is also consistent with the biostratigraphically assigned middle Eocene age of the Ballena Formation. The youngest significant age peak from sample CCa1 spans 40–46 Ma, with nearly identical Σ, τ and δ maximum ages at ca. 43 Ma; these ages are consistent with the ca. 39 Ma biostratigraphic age assigned to Member A of the Cerro Colorado Formation. A single 33.9 ± 1.2 Ma zircon analyzed from this sample is significantly younger than the assigned biostratigraphic age, which we opt to disregard in light of stratigraphic relationships and previous biostratigraphy. The youngest significant detrital-zircon peak from sample CCc1 spans 65–82 Ma, with δ, τ and Σ ages at 72.0 ± 1.3, 74.9 ± 1.3, and ca. 76 Ma, respectively. As with CCa1, a single earliest Oligocene zircon (33.2 ± 3.4 Ma) is significantly younger than the latest middle Eocene biostratigraphic age assigned to Member C of the Cerro Colorado Formation. We disregard this single-grain ϕ age and interpret the depositional age of this sample at ca. 38.5 Ma, in line with biostratigraphic estimates.

Sample CCd1 contains a detrital-zircon age peak spanning 77–95 Ma, with δ and τ ages of 78.2 ± 2.1 and 80.3 ± 4.3 Ma, respectively, the former of which is coincident with the Σ age of ca. 78 Ma. All of these ages are significantly older than the well-constrained late Eocene (34.3–36 Ma) biostratigraphic age of Member D of the Cerro Colorado Formation, which we use in our interpretations below. The youngest significant age peak in sample MC1 spans 150–190 Ma, although it also contains three younger ϕ-age peaks, two of which are derived from a single grain (75.0 ± 2.2 and 106.6 ± 2.2 Ma), and one that is derived from two grains (86.8 ± 2.8 Ma). All of these ages are significantly older than the biostratigraphically constrained earliest Oligocene age (30–32 Ma) for the Estancia Maria Cristina beds, which we use for our interpretations. The youngest significant peak for sample PG1 spans ca. 19–31 Ma, with a statistically robust δ age of

Fig. 4. Histograms and probability plots of detrital-zircon U/Pb age populations from single eastern Magallanes foreland basin samples analyzed in this study. Plots are arranged with the oldest sampled stratigraphic unit at the bottom and the youngest unit at the top. Left column depicts age distributions of all grains younger than 800 Ma: the numbers in parentheses indicate the number of analyzed grains that are older than 800 Ma. Right column depicts a close-up of the post-Triassic portion of the probability distributions: the boxed numbers in the upper left corner of each plot indicate the number and percentage of grains that fall within plotted range. See supplementary material for all data and metadata. The patterned polygons depict the dominant age ranges of the batholith, metamorphic complex and Jurassic volcanic sources (Fig. 3) for comparison to the foreland basin detrital-zircon age distributions.

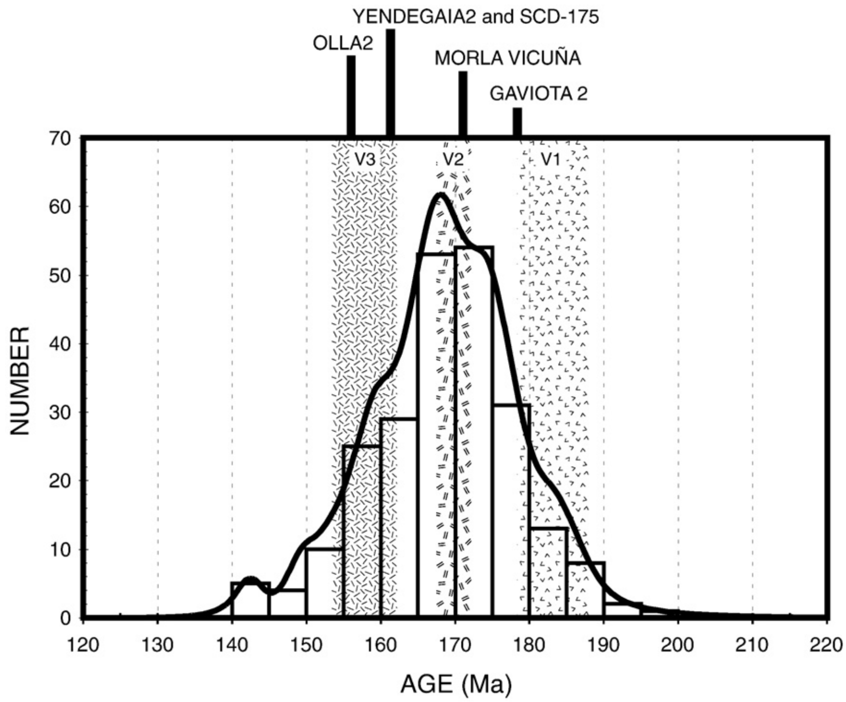

Fig. 5. Zircon U/Pb age distribution of all Jurassic grains from the eastern Magallanes foreland basin samples analyzed in this study. The magmatic phases (V1, V2, V3) of Pankhurst et al. (2000) associated with break-up of Gondwana are plotted along with geochronology of Jurassic rocks exposed in the southernmost Andes. Gaviota 2 and Morla Vicuña are from Pankhurst et al. (2000), SCD-175 is from Mukasa and Dalziel (1996) and OLLA2 and YENDEGAIA2 are reported in this study.

26.27 ± 0.63 which we use instead of its slightly older 34.0–26.5 Ma (early Oligocene) biostratigraphic age estimate.

5.2. Age distributions

In Fig. 2 and Table S2, we report the composite detrital-zircon U/Pb age probability distribution constructed from all the eastern Magallanes foreland basin detrital zircons analyzed in this study, and compare the resulting age distribution with the composite age distributions of candidate source rocks described in Section 2. These candidate sources include the south Patagonian batholith (Rolando et al., 2002; Hervé et al., 2007); Jurassic volcanic strata and related intrusives from southern South America and the Antarctic Peninsula associated with the break-up of Gondwana (Féraud et al., 1999; Pankhurst et al., 2000); and metasedimentary complexes from the Patagonian Andes (Hervé and Fanning, 2003; Hervé et al., 2003; Augustsson et al., 2006). The latter are plotted adjacent to sample SONIA1 collected from the Cordillera Darwin metamorphic complex of the Fuegian Andes (this study). In Table S2 and Fig. S2 we report the crystallization ages of zircon collected from the orthogneiss samples OLLA2 and YENDEGAIA2.

Sample SONIA1 ($n = 93$) contains a large 280–310 Ma zircon peak, comprising 27% of the sample's analyzed grains. Less defined peaks spanning 450–500 Ma and 550–630 Ma are comparatively prominent amongst diffuse populations of 320–630 Ma and 700–1100 Ma zircons that constitute 36% and 25% of the analyzed grains, respectively (Fig. 2A). The remaining SONIA1 zircons (nine grains, 10% of the total) have broadly distributed, isolated ages between 1.4 and 3.5 Ga (Table S2). Samples OLLA2 and YENDEGAIA2 ($n = 20$ each) contain unimodal zircon age populations that suggest crystallization at 156.7 ± 1.9 (95% conf., MSWD = 1.8) and 160.4 ± 2.4 Ma (95% conf., MSWD = 0.86), respectively.

The composite eastern Magallanes foreland basin detrital-zircon distribution (Fig. 2; $N = 11$, $n = 1043$) analyzed in this study is dominated by Cretaceous–Paleogene (53%) and Jurassic zircons (23%), with subordinate contributions from 200–600 Ma (18%), and older populations (6%). Within the post-Triassic population of the analyzed grains, prominent peaks are centered on ca. 75 Ma and 100 Ma, approximately coincident with recognized peaks in the sampled granitoids of the south Patagonian batholith (Rolando et al., 2002; Hervé et al., 2007), and on ca. 170 Ma, coincident with the peak of Jurassic magmatism recognized in the silicic large igneous province of southern South America and the Antarctic Peninsula (Fig. 2B; Féraud et al., 1999; Pankhurst et al., 2000). Within the 200–600 Ma population of grains, prominent, peaks are centered on ca. 275 Ma and 470 Ma, with lesser peaks at 360–420 Ma and ca. 560 Ma (Fig. 2A). Older, broad, and less prominent probability peaks occur at ca. 630 Ma and 1080 Ma, with additional broad, small and/or isolated sub-populations from 0.7–0.9 Ga, 1.2–1.3 Ga, 1.5–1.7 Ga, 1.8–2.0 Ga and ca. 2.7 Ga (Fig. 2A, Table S2).

The distributions of detrital-zircon age populations from individual eastern Magallanes foreland basin samples are illustrated in Fig. 4. Individual samples can be subdivided into three groups based on their age distributions: (1) those largely dominated by Cretaceous–Paleogene populations (72–91% of grains, mean of 80%); (2) a single sample (CCc1) with comparable Jurassic (42%), Cretaceous–Paleogene (30%) and older (28%) populations; and (3) those with significantly larger Jurassic (35–65%, mean of 49%) than Cretaceous–Paleogene (6–20%, mean of 10%) populations, accompanied by significant pre-Jurassic populations (15–60%, mean of 41%). Group (1) samples have depositional ages between ca. 75 and 39 Ma. The CCc1 sample was deposited at ca. 38.5 Ma. The Group (3) samples have depositional ages between ca. 35 and 26 Ma (Table S1).

6. Interpretations

6.1. Sediment provenance of the Cordillera Darwin complex protolith

The detrital-zircon composition of sample SONIA1 from the southern Cordillera Darwin metamorphic complex (Fig. 2A) is similar to that of metasedimentary units exposed in the hinterland of the Patagonian Andes (Hervé and Fanning, 2003; Hervé et al., 2003; Augustsson et al., 2006), and suggests a mixed provenance from the Gondwanide, Famatinian, Pampean and Sunsás belts (see Section 2.2.1). Although the dominant age probability peak in SONIA1 (ca. 295 Ma) slightly post-dates that of the composite probability plot determined for the other Andean metamorphic complexes (ca. 280 Ma), the overall range of ages and the morphology of late Paleozoic, early Paleozoic and Proterozoic age probability peaks are remarkably similar, especially when considering the small number of SONIA1 grains that define the early Paleozoic and Proterozoic peaks. These results suggest that at the level of analysis employed herein, the Cordillera Darwin and Patagonian Andes metamorphic complex samples have sufficiently similar detrital-zircon compositions to employ the latter's more robust composite age probability distribution for interpreting recycled sediment contributions from Cordillera Darwin complex in the composite and individual age probability distributions of the Magallanes foreland basin samples.

6.2. Bulk sediment provenance of the eastern Magallanes foreland basin

The bulk detrital-zircon composition of sampled eastern Magallanes foreland basin strata is consistent with derivation dominantly from the Cretaceous–Neogene Patagonian–Fuegian magmatic arc, the Jurassic volcanic and plutonic rocks associated with Gondwana break-up, and contributions from southern Andean metamorphic complexes that bear mainly pre-Jurassic zircons (Fig. 2).

Although Late Jurassic zircons occur in the south Patagonian batholith (Hervé et al., 2007), the age distribution of Jurassic zircons in the composite eastern Magallanes foreland basin is more similar to that of the volcanic and plutonic rocks associated with the break-up of Gondwana (Fig. 2B). Hence, we interpret Cretaceous and Paleogene zircons occurring in the Magallanes foreland basin as having been derived from the Patagonian–Fuegian magmatic arc, and Jurassic zircons having been derived from the Tobífera/Lemaire Formation volcanics and associated plutons, which are currently exposed in hinterland thrust sheets of the Fuegian Andes (Fig. 1). Similar Jurassic magmatic rocks are also exposed in the Deseado & North Patagonian Massifs that reside 700 and 2000 km north of the study area, respectively, and provide an alternative source for the Jurassic zircons that occur in our samples. Pankhurst et al. (2000) interpreted the age distribution of Jurassic volcanic and granitic rocks in southern South America and the Antarctic Peninsula as the result of three separate phases of Jurassic magmatism (V1, V2 and V3), which they suggest indicate a southwestward-younging trend that could offer an opportunity to confirm or refute our interpretation of the source of Jurassic zircons in eastern Magallanes basin strata. However, the age distribution of all Jurassic zircons analyzed from our foreland basin samples spans the entirety of the three phases (Fig. 5). In light of our new U/Pb data from Jurassic Cordillera Darwin felsic/silicic orthogneisses (OLLA2 and YENDEGAIA2) and previous high-precision geochronology of Jurassic rocks from the southern Cordillera Darwin (Mukasa and Dalziel, 1996), Canal Morla Vicuña, and from the Gaviota 2 borehole in the Magallanes basin subsurface (Pankhurst et al., 2000), it appears that felsic/silicic Jurassic igneous rocks exposed in the southernmost Andes also represent contributions from all three of the Pankhurst et al. (2000) volcanic phases. It is therefore more probable that the Jurassic zircons in the eastern Magallanes basin sandstones were derived from the Fuegian Andes than from the distant massifs. This interpretation is supported by paleocurrent and seismic stratigraphy data (Biddle et al., 1986; Galeazzi, 1998) from the Campanian–Maastrichtian Bahía Thetis Formation and equivalent deposits (Martinioni et al., 1999; Olivero et al., 2003) and the Paleogene sandstones of the Tres Amigos Formation, Río Claro Group, Punta Torcida Formation and Leticia–Ballena–Cerro Colorado Formations and equivalent deposits (Torres Carbonell et al., 2008), which demonstrate across-axis transport of sediment derived from the Fuegian Andes. This interpretation is further bolstered by sandstone petrographic data indicating the foliated nature of Tobífera/Lemaire clasts in eastern Magallanes basin sediments (Olivero et al., 2002). Whereas these units are foliated in the Fuegian Andes, Jurassic volcanics in the Deseado Massif do not have these metamorphic textures.

In light of these sediment transport observations and the lack of a suitable alternate source, we thus interpret pre-Jurassic zircons occurring in the eastern Magallanes foreland basin samples as having been derived from the Cordillera Darwin metamorphic complex in the Fuegian Andes hinterland (Fig. 2A).

6.3. Kinematic history of the Fuegian Andes as indicated by detrital-zircon sediment provenance

We apply the provenance interpretations described in Section 6.2 to the detrital-zircon age distributions of individual eastern Magallanes foreland basin samples in order to reconstruct the Late Cretaceous to Oligocene compositional and kinematic evolution of the Fuegian Andes.

6.3.1. Evolution of eastern Magallanes foreland basin sediment provenance

Based on the dominance of Cretaceous and Paleogene detrital zircons in our Group (1) samples (Fig. 4), we interpret the Upper Cretaceous through middle Eocene strata of the eastern Magallanes foreland basin as having been derived almost entirely from the Patagonian–Fuegian magmatic arc. The significant differences between each sample's depositional age and that of its most abundant detrital-zircon sub-population preclude the possibility that the abundances of arc-aged zircons were inflated by syndepositional magmatism, which combined with the broad range of Cretaceous and Paleogene zircon ages suggests that sediment was derived from diverse rocks within the magmatic arc. However, given the similar age distributions of Cretaceous zircons in many of the Group (1) samples, and independent evidence of syndepositional deformation in the Magallanes foreland thrust belt (Ghiglione and Ramos, 2005), it is possible that some of the arc-aged zircons in these samples were recycled from wedge-top strata of the proximal Magallanes foreland basin. Finally, the relative dearth of Jurassic and pre-Triassic zircons in these samples preclude significant sediment contribution from Tobífera/Lemaire-bearing thrust sheets or the Cordillera Darwin complex that occur in the more hinterland parts of the Fuegian Andes.

In contrast to the protracted dominance of arc-derived sediment in the Upper Cretaceous to middle Eocene Group (1) samples, the sudden increase in the abundance of Jurassic zircons in the CCc1 and Group (3) samples (Fig. 4) suggests late middle Eocene (ca. 39 Ma) exhumation of the Tobífera/Lemaire Formations in proximity to the Magallanes foreland basin. Although not as uniformly abundant, the coeval increase in the abundance of pre-Triassic zircons also suggests sediment derivation from metasedimentary strata of the Cordillera Darwin complex. These increases coincide with a decrease in the relative abundance of Cretaceous and younger zircons, from ~80% in the Group (1) samples, to 30% in sample CCc1, to ~10% in the Group (3) samples, suggesting progressive elimination of the Patagonian–Fuegian arc as a sediment source for the eastern Magallanes foreland basin, despite its well-documented Paleogene and Neogene activity (Hervé et al., 2007). Together, these three provenance changes record a fundamental reorganization of the sediment sources to the Magallanes foreland basin in the late middle Eocene.

6.3.2. Model

We propose a generalized kinematic model (Fig. 6) that we consider the most parsimonious explanation for the observed sediment provenance changes while maintaining consistency with independent constraints for the evolution of the Fuegian Andes. Our data suggest that sediment was largely derived from the Patagonian–Fuegian magmatic arc beginning with the onset of crustal thickening and foreland basin subsidence in the Late Cretaceous (Biddle et al., 1986). Derivation of this sediment from the arc requires (a) the orogen's drainage divide was positioned at least as outboard as the magmatic arc, and (b) a sediment pathway connected this hinterland sediment source with the Magallanes foreland basin. This configuration appears to have persisted until the late middle Eocene, although

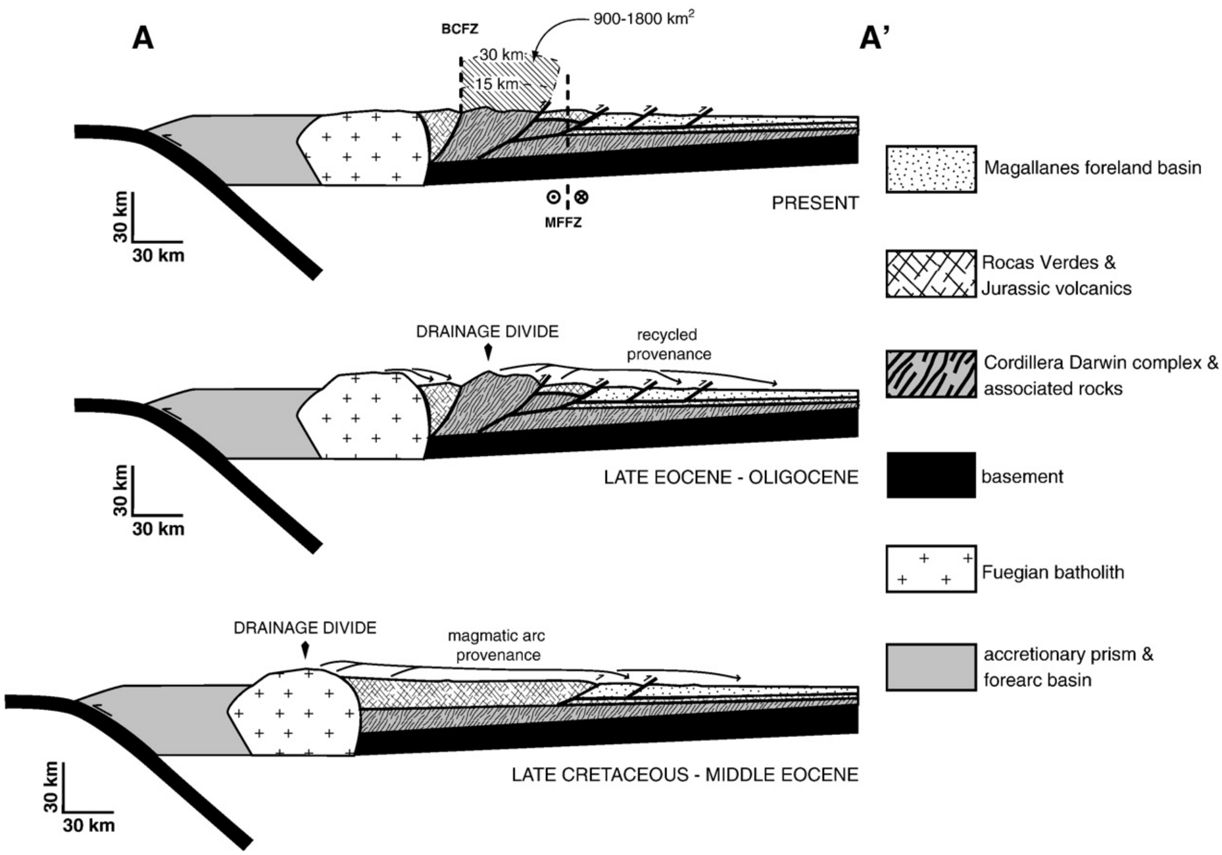

Fig. 6. Interpreted kinematic history of the Fuegian Andes based on detrital-zircon provenance data collected from Upper Cretaceous to Oligocene strata of the eastern Magallanes foreland basin of Tierra del Fuego. The line of the cross-section is depicted in Fig. 1.

the occurrence of occasional, small populations of pre-Triassic zircons in some Group (1) samples is consistent with contributions from rocks of the partially exhumed Cordillera Darwin complex. Alternatively, it is possible these pre-Triassic zircons were derived from inherited zircons within the Patagonian–Fuegian magmatic arc.

In contrast to the 30 million year history of magmatic arc sediment provenance observed in the Upper Cretaceous through middle Eocene strata of the eastern Magallanes basin, we interpret our latest middle Eocene and younger samples as evidence for rapid exhumation of the hinterland of the Fuegian Andes. In light of deformational evidence from structural relationships (Klepeis, 1994a), thermochronology (Nelson, 1982; Kohn et al., 1995; Gombosi et al., 2009) and the stratigraphic record of flexural subsidence (Biddle et al., 1986; Ghiglione and Ramos, 2005), this exhumational event is most consistent with crustal shortening and associated rock-uplift of thrust sheets intervening the foredeep of the Magallanes foreland basin and the Patagonian–Fuegian batholith (Figs. 1C and 6). We envision such deformation simultaneously (1) shifting the orogenic drainage divide inboard, thereby damming the sediment pathway between magmatic arc and foreland basin, and (2) prominently exhuming the Cordillera Darwin complex and Tobífera/Lemaire Formations in thrust sheets now widely exposed in the Fuegian Andes hinterland, thereby recycling their contents into the Magallanes foreland basin. Our provenance data suggest that this configuration persisted until the late Oligocene, after which the convergent tectonic regime of the Fuegian Andes gave way to sinistral deformation along the Magallanes–Fagnano and possibly Beagle Channel fault zones (MFFZ and BCFZ respectively; Klepeis, 1994b).

7. Discussion

The earliest Oligocene glaciation of Antarctica has been frequently attributed to the tectonic opening of Drake Passage and the resulting establishment of the ACC (Barker and Burrell, 1977). However, several recent efforts challenge a causal relationship between marine gateway opening and polar glaciation, including those that favor alternative glaciation mechanisms (DeConto and Pollard, 2003; Pagani et al., 2005; Huber and Nof, 2006) and others that suggest a mismatch between the timing of Antarctic glaciation and ACC development (Barker, 2001; Pfuhl and McCave, 2005; Lyle et al., 2007; Koenitz et al., 2008). Evaluation of this 'polar gateway' hypothesis requires an understanding of the temporal relationships between Scotia Arc plate kinematics, penetration of Pacific seawater through Drake Passage, and the growth of ice sheets on Antarctica. Towards these ends, our new detrital-zircon provenance data from the eastern Magallanes foreland basin provide insight into the kinematics of the western part of the northern Scotia arc.

In Fig. 7, we plot the temporal relationships between marine proxy data indicating the Oi-1 glaciation of Antarctica (Zachos et al., 2001) and ocean circulation through Drake Passage (Scher and Martin, 2006) in conjunction with interpreted Scotia seafloor ages (Barker and Burrell, 1977; Barker, 2001; Eagles et al., 2005) and the relative abundance of the interpreted zircon provenance populations in each of the studied eastern Magallanes foreland basin samples (this study).

The reconstruction of marine $\delta^{18}O$ isotope ratios from benthic foraminifera (Zachos et al., 2001) records the combined effects of global ice-volume and ocean temperature variations since the end of the Cretaceous. At least one-half of the dramatic >1.0‰ positive isotopic shift that occurs in the earliest Oligocene is associated with ice-volume increase (Lear et al., 2000), which along with coeval evidence of ice-rafted debris and clay mineralogy changes in the Southern Ocean is widely interpreted to record the Oi-1 glaciation of Antarctica at ca. 34 Ma (Zachos et al., 2001).

Interpretation of magnetic seafloor anomalies and gravity data from the Scotia Sea suggest that seafloor spreading was active by at least chron C8 (ca. 26.5 Ma; Barker and Burrell, 1977; Barker, 2001;

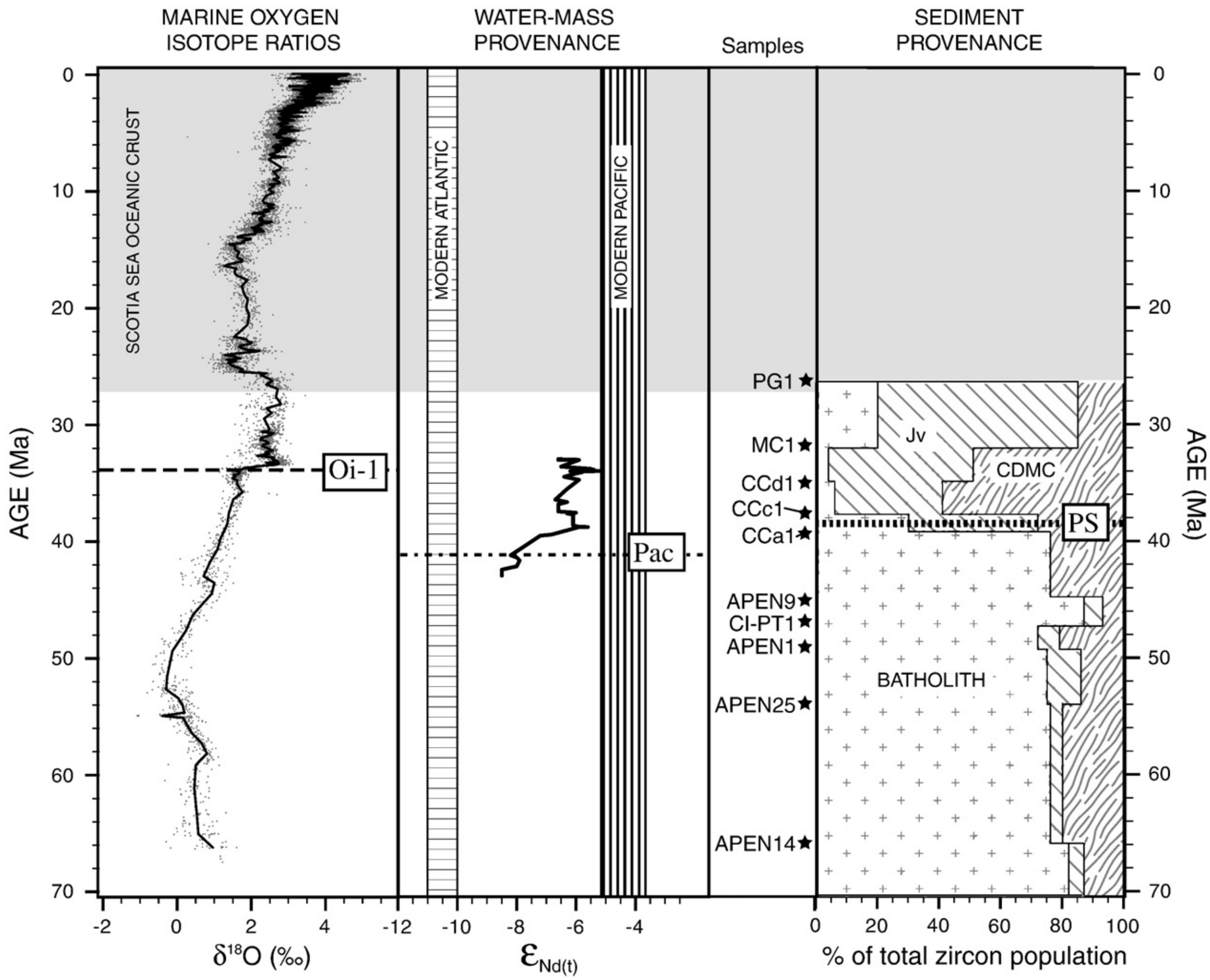

Fig. 7. Comparison of global benthic foraminifera $\delta^{18}O$ (Zachos et al., 2001) and Atlantic-sector Southern Ocean fish-tooth ε_{Nd} (Scher and Martin, 2006) isotope values with eastern Magallanes foreland basin detrital-zircon provenance data collected as part of this study. "Oi-1" depicts the onset of the Antarctic glaciation that occurred at the Eocene–Oligocene transition. "Pac" depicts the onset of the transition from Atlantic towards Pacific type water-mass compositions in the Atlantic sector of the Southern Ocean (Scher and Martin, 2006). "PS" indicates the onset of the dramatic sediment provenance shift recognized in the eastern Magallanes foreland basin. BATHOLITH: detrital zircons with ages consistent with derivation from the Fuegian batholith. Jv: detrital zircons with ages consistent with derivation from the Jurassic-aged Tobífera Formation volcanics and associated Darwin suite of granitoids. CDMC: detrital-zircons with ages consistent with derivation from the Cordillera Darwin metamorphic complex.

Eagles et al., 2005). Evidence of incoherent displacement in the western Scotia Sea suggest that spreading may have begun earlier (chron C10: ca. 29 Ma: Lodolo et al., 1997), although the challenges of magnetic anomaly interpretation of such small regions (Barker, 2001) leaves open the possibility of other age interpretations for many seafloor fragments in the Scotia Sea (e.g., Eagles et al., 2006).

In contrast to geophysical interpretations that favor a Middle to Late Oligocene onset of Scotia Sea tectonics, Nd isotope data collected from Eocene–Oligocene fossil fish teeth in the south Atlantic Ocean reveal a ~2‰ positive shift in seawater $\varepsilon_{Nd}(t)$ beginning at ca. 42–39 Ma, which is consistent with the influx of the more isotopically juvenile Pacific waters through Drake Passage into the Atlantic sector of the Southern Ocean beginning at that time (Scher and Martin, 2006). This geochemical proxy evidence has been more recently integrated with basin and tectonic models to suggest a protracted opening of Drake Passage beginning with shallow opening as early as ca. 50 Ma (Livermore et al., 2007; Ghiglione et al., 2008; Lagabrelle et al., 2009).

As described in Section 6 above, our detrital-zircon data record a fundamental sediment provenance shift in the eastern Magallanes foreland basin at ca. 39 Ma as indicated by the remarkably rapid decrease in relative abundance of Cretaceous–Paleogene detrital zircons and concomitant increase of Jurassic and Paleozoic–Neoproterozoic populations (Figs. 4 & 7). These results suggest a dramatic reorganization of the Fuegian Andes orogen that is most parsimonious and consistent with middle Eocene shortening and exhumation of the orogenic hinterland (this study: Fig. 6), which is independently supported by new thermochronometry data from the Cordillera Darwin complex and adjacent regions (Gombosi et al., 2009) applied to documented structural relationships (e.g., Klepeis, 1994a). This interpreted kinematic reorganization demonstrates a temporal relationship between Fuegian Andes deformation and the water-mass provenance evidence of the opening of the adjacent Drake Passage from Scher and Martin (2006).

Whereas a temporal relationship alone is insufficient to ascribe causality, it is difficult to imagine that dramatic shortening and exhumation in the Fuegian Andes would not affect the adjacent and coevally developing Drake Passage. The assessment of a genetic relationship between these apparently coeval processes requires the integrative analysis of numerous geophysical, geologic and geochemical data, vital components of which are currently being collected. While these considerations are beyond the scope of this paper, we suggest that Eocene counterclockwise vertical-axis rotation of the Fuegian Andes to form the Patagonian orocline would account for: (a) the numerous indications of greater shortening in the Fuegian Andes than in the Patagonian Andes as described in Section 1, (b) the dramatic sediment provenance change (this study) associated with exhumation of the Cordillera Darwin and associated thrust sheets in the hinterland of the Fuegian Andes (Nelson, 1982; Kohn et al., 1995; Gombosi et al., 2009), and (c) rotative opening of the Drake Passage polar gateway sufficient to allow the flow of isotopically juvenile Pacific water-mass into the isotopically evolved southern Atlantic Ocean (Scher and Martin, 2006). Such oroclinal bending also eliminates the need for the geologically dissatisfying 'cuspate' model of pre-Drake Passage South America–Antarctic Peninsula reconstructions (Dalziel, 1983). Despite these advantages of interpreting Eocene oroclinal bending in the Fuegian Andes, paleomagnetic and structural evaluation of the required vertical-axis rotations is currently equivocal (cf. Diraison et al., 2000; Kraemer, 2003; Ghiglione and Cristallini, 2007; Rapalini, 2007), and is further complicated by challenges of identifying an appropriate driving mechanism for such differential shortening and oroclinal bending.

While an open marine gateway between South America and Antarctica is required for the development of the ACC, evidence of a zenith of Eocene tectonic activity in the Scotia arc alone is insufficient to constrain the ACC onset that may have caused or contributed to Oi-1 glaciation because of the significant sill depths required to allow such circulation (Livermore et al., 2007). However, the ~5 Myr lag between the timing of the provenance shift recorded herein (ca. 39 Ma) and the Oi-1 glaciation (ca. 34 Ma) may have allowed time for the development of sufficient sill depths. The sediment provenance data and kinematic interpretations presented herein are temporally consistent with independent evidence of a middle Eocene onset of Drake Passage opening (Scher and Martin, 2006). Whether sufficient opening and associated subsidence occurred to allow ACC development in time for the Oi-1 glaciation remains to be seen. Considering the ACC's dominant influence upon modern global ocean circulation and temperature distribution (Barker, 2001), constraining the timing and nature of its onset remains vitally important. It appears that at least one part of the gateway's development involved the Eocene kinematics of the Fuegian Andes.

8. Conclusions

1. U/Pb detrital-zircon data from a quartzite in the Cordillera Darwin metamorphic complex of the Fuegian Andes hinterland reveal an age distribution that resembles the composite age distribution of lower grade metasedimentary complexes reported from the Patagonian Andes hinterland, suggesting a genetic relationship between the complexes.
2. U/Pb geochronology from felsic/silicic orthogneisses preserved in the southern Cordillera Darwin complex suggests Late Jurassic magmatism in the southernmost Andes, in addition to Early and Middle Jurassic magmatism recognized previously. Together these rocks suggest a protracted involvement of southernmost South America in the break-up of Gondwana.
3. The bulk U/Pb age distributions from >1100 detrital zircons collected from upper Cretaceous–Oligocene strata of the eastern Magallanes basin suggest (1) derivation of Cretaceous–Paleogene components from the Patagonian–Fuegian magmatic arc, (2) derivation of Jurassic grains from volcanic and plutonic rocks associated with the break-up of Gondwana now exposed in the hinterland thrust sheets of the Fuegian Andes, and (3) derivation of abundant Paleozoic and Proterozoic zircons from metasedimentary rocks of the Cordillera Darwin complex.
4. Upper Cretaceous through late middle Eocene sandstones collected from the eastern Magallanes foreland basin are dominated by zircons derived from the Patagonian–Fuegian magmatic arc, whereas upper Eocene and Oligocene strata are dominated by zircon populations consistent with derivation from Jurassic igneous rocks and the Cordillera Darwin complex, both of which are widely exposed in the Fuegian Andes hinterland. The dramatic provenance shift recorded at ca. 39 Ma is consistent with rapid uplift and exhumation in the Fuegian Andes hinterland recognized in recent thermochronometry studies. Marine geochemical evidence for near contemporaneous opening of the Drake Passage suggests that the kinematic history of the Fuegian Andes may have played an important role in the development of the marine gateway and the subsequent Antarctic circumpolar current that is widely recognized to thermally isolate Antarctica from tropical gyres.

Acknowledgments

This research was primarily supported by International Polar Year grant ANT-0732995 to DLB from the U.S. National Science Foundation Office of Polar Programs. Additional funding came from NSF grant EAR-0443387 to GG, and a University of South Carolina Research & Productive Scholarship grant to DLB and by grant PICTO 36315 ANPCyT-FONCyT to EBO. Carlos Pastoriza granted access to Estancia Río Apen. H. Scher provided important paleooceanographic insight. M. Ghiglione contributed a preprint and guidance in the Punta Gruesa and C. Irigoyen regions. D. Gombosi and A. Moragues provided field assistance. J. Davis provided sample preparation assistance. V. Valencia, A. Pullen, and M. Baker provided instrument support at the Arizona LaserChron Center.

Appendix A. Supplementary data

Supplementary data associated with this article can be found, in the online version, at doi:10.1016/j.epsl.2009.05.014.

References

Andersen, T., 2005. Detrital zircons as tracers of sedimentary provenance: limiting conditions from statistics and numerical simulation. Chem. Geol. 216, 249–270.
Augustsson, C., Munker, C., Bahlburg, H., Fanning, C.M., 2006. Provenance of late Palaeozoic metasediments of the SW South American Gondwana margin: a combined U–Pb and Hf-isotope study of single detrital zircons. J. Geol. Soc. 163, 983–995.
Barker, F., 2001. Scotia Sea regional tectonic evolution: implications for mantle flow and palaeocirculation. Earth Sci. Rev. 55, 1–39.
Barker, F., Burrell, J., 1977. The opening of Drake Passage. Mar. Geol. 25, 15–34.
Biddle, K.T., Uliana, M.A., Mitchum, J.R., Fitzgerald, M.G., Wright, R.C., 1986. The stratigraphic and structural evolution of the central and eastern Magallanes Basin, southern South America, in Allen, P.A., Homewood, P. (Eds.), Foreland Basins (Special Publication of the International Association of Sedimentologists 8). InBlackwell, Oxford, pp. 41–61.
Buatois, L.A., Camacho, H.H., 1993. Geología del sector nororiental del Lago Fagnano, Isla Grande de Tierra del Fuego. Rev. Asoc. Geol. Argent. 48, 109–124.
Cunningham, W.D., 1994. Uplifted ophiolitic rocks on Isla Gordon, southernmost Chile: Implications for the closure history of the Rocas Verdes marginal basin and the tectonic evolution of the Beagle Channel region. J. South Am. Earth Sci. 7, 135–148.
Dalziel, I.W.D.,1983. The evolution of the Scotia Arc: a review, in Oliver, R.L., James, P.R., Jago, J.B. (Eds.), Antarctic Earth Science. Cambridge University Press, London, pp. 283–298.
Dalziel, I.W.D., Brown, R.L., 1989. Tectonic denudation of the Darwin metamorphic core complex in the Andes of Tierra del Fuego, southernmost Chile: implications for Cordilleran orogenesis. Geology 17, 699–703.
Dalziel, I.W.D., Elliot, D.H., 1971. Evolution of the Scotia Arc. Nature 233, 246–252.
Dalziel, I.W.D., de Wit, M.J., Palmer, K.F., 1974. Fossil marginal basin in the southern Andes. Nature 250, 291–294.
DeCelles, P.G., Carrapa, B., Gehrels, G.E., 2007. Detrital zircon U–Pb ages provide new provenance and chronostratigraphic information from Eocene synorogenic deposits in northwestern Argentina. Geology 35, 323–326.
DeCelles, P.G., Pile, H.T., Coogan, J.C., 1993. Kinematic history of the Meade Thrust based on provenance of the Bechler Conglomerate at Red Mountain, Idaho, Sevier thrust belt. Tectonics 12, 1436–1450.
DeConto, R.M., Pollard, D., 2003. Rapid Cenozoic glaciation of Antarctica induced by declining atmospheric CO_2. Nature 421, 245–249.
Diraison, M., Cobbold, P.R., Gapais, D., Rossello, A.R., Le Corre, C., 2000. Cenozoic crustal thickening, wrenching and rifting in the foothills of the southernmost Andes. Tectonophysics 316, 91–119.
Dott, R.H., Winn Jr, R.D., Smith, C.H.L., 1982. Relationship of Late Mesozoic and Early Cenozoic sedimentation to the tectonic evolution of the southernmost Andes and the Scotia Arc, in Craddock, C. (Ed.), Antarctic Geoscience. Univ. Wisconsin Press, Madison, pp. 193–202.
Eagles, G., Livermore, R.A., Fairhead, J.D., Morris, P., 2005. Tectonic evolution of the west Scotia Sea. J. Geophys. Res.-Solid Earth 110. doi:10.1029/2004JB003154.
Eagles, G., Livermore, R., Morris, P., 2006. Small basins in the Scotia Sea: the Eocene Drake Passage gateway. Earth Planet. Sci. Lett. 242, 343–353.
Faundez, V., Herve, F., Lacassie, J.P., 2002. Provenance and depositional setting of pre-Late Jurassic turbidite complexes in Patagonia, Chile. N. Z. J. Geol. Geophys. 45, 411–425.

Fedo, C.M., Sircombe, K.N., Rainbird, R.H., 2003. Detrital-zircon analysis of the sedimentary record, in Hanchar, J.M., Hoskin, P. (Eds.), Zircon: Experiments, Isotopes, and Trace Element Investigations: Mineralogical Society of America, Reviews in Mineralogy, vol. 53, pp. 277–303.
Féraud, G., Alric, Fornari, M., Bertrand, H., Haller, M., 1999. $^{40}Ar/^{39}Ar$ dating of the Jurassic volcanic province of Patagonia: migrating magmatism related to Gondwana break-up and subduction. Earth Planet. Sci. Lett. 172, 83–96.
Fildani, A., Hessler, A.M., 2005. Stratigraphic record across a retroarc basin inversion: Rocas Verdes–Magallanes Basin, Patagonian Andes, Chile. Geol. Soc. Amer. Bull. 117, 1596–1614.
Fildani, A., Cope, T.D., Graham, S.A., Wooden, J.L., 2003. Initiation of the Magallanes foreland basin: timing of the southernmost Patagonian Andes orogeny revised by detrital-zircon provenance analysis. Geology 31, 1081–1084.
Galáz, G., Hervé, F., Calderón, M., 2005. Metamorfismo y deformación de la Formación Tobífera en la cordillera Riesco, región de Magallanes, Chile: evidencias para su evolución tectónica. Rev. Asoc. Geol. Argent. 60, 762–774.
Galeazzi, J.S., 1998. Structural and stratigraphic evolution of the western Malvinas Basin, Argentina. AAPG Bull. 82, 596–636.
Gehrels, G., Valencia, V.A., Pullen, A., 2006. Detrital zircon geochronology by laser-ablation multicollector ICPMS at the Arizona Laserchron Center, in: Emerging Opportunities. Paleontological Society Short Course, Philadelphia, PA, pp. 67–76.
Ghiglione, M.C., Cristallini, E.O., 2007. Have the southernmost Andes been curved since Late Cretaceous time? An analog test for the Patagonian Orocline. Geology 35, 13–16.
Ghiglione, M.C., Ramos, V.A., 2005. Progression of deformation and sedimentation in the southernmost Andes. Tectonophysics 405, 25–46.
Ghiglione, M.C., Yagupsky, D., Ghidella, M., Ramos, V.A., 2008. Continental stretching preceding the opening of the Drake Passage: evidence from Tierra del Fuego. Geology 36, 643–646.
Gombosi, D.J., Barbeau, D.L., Garver, J.I., 2009. New Thermochronometric Constraints on the Rapid Paleogene Exhumation of the Cordillera Darwin Complex and Related Thrust Sheets in the Fuegian Andes. accepted pending revisions Terra Nova.
Hervé, F., Fanning, C.M., 2003. Early Cretaceous subduction of continental crust at the Diego de Almargo archipelago, southern Chile. Episodes 26, 285–289.
Hervé, F., Fanning, C.M., Pankhurst, R.J., 2003. Detrital zircon age patterns and provenance of the metamorphic complexes of southern Chile. J. South Am. Earth Sci. 16, 107–123.
Hervé, F., Pankhurst, R.J., Fanning, C.M., Calderón, M., Yaxley, G.M., 2007. The South Patagonian batholith: 150 My of granite magmatism on a plate margin. Lithos 97, 373–394.
Horton, B.K., Hampton, B.A., LaReau, B.N., Baldellón, E., 2002. Tertiary provenance history of the northern and central Altiplano (central Andes, Bolivia): a detrital record of plateau-margin tectonics. J. Sediment. Res. 72, 711–726.
Huber, M., Nof, D., 2006. The ocean circulation in the southern hemisphere and its climatic impacts in the Eocene. Palaeogeogr. Palaeoclimatol. Palaeoecol. 231, 9–28.
Kennett, J.P., 1977. Cenozoic evolution of Antarctic glaciation, the circum-Antarctic Ocean, and their impact on global paleoceanography. J. Geophys. Res. 82, 3843–3860.
Klepeis, K.A., 1994a. Relationship between uplift of the metamorphic core of the southernmost Andes and the shortening in the Magallanes foreland fold and thrust belt, Tierra del Fuego, Chile. Tectonics 13, 882–904.
Klepeis, K.A., 1994b. The Magallanes and Deseado fault zones: major segments of the South American–Scotia transform plate boundary in southernmost South America, Tierra del Fuego. J. Geophy. Res. 99, 22001–22014.
Koenitz, D., White, N., McCave, I.N., Hobbs, R., 2008. Internal structure of a contourite drift generated by the Antarctic Circumpolar Current. Geochem. Geophys. Geosyst. 9. doi:10.1029/2007GC001799.
Kohn, M.J., Spear, F.S., Harrison, M.T., Dalziel, I.W.D., 1995. $^{40}Ar/^{39}Ar$ geochronology and P–T–t paths from the Cordillera Darwin metamorphic complex, Tierra del Fuego, Chile. J. Metamorph. Geol. 13, 251–270.
Kraemer, E., 2003. Orogenic shortening and the origin of the Patagonian orocline, 56°S. J. South Am. Earth Sci. 15, 731–748.
Lagabrelle, Y., Goddéris, Y., Donnadieu, Y., Malavieille, J., Suarez, M., 2009. The tectonic history of Drake Passage and its possible impacts on global climate. Earth Planet. Sci. Lett. 279, 197–211.
Lear, C.H., Elderfield, H., Wilson, P.A., 2000. Cenozoic deep-sea temperatures and global ice volumes from Mg/Ca in benthic foraminiferal calcite. Science 287, 269–272.
Livermore, R., Hillenbrand, C., Meredith, M., Eagles, G., 2007. Drake Passage and Cenozoic climate: an open and shut case? Geochem. Geophys. Geosyst. 8. doi:10.1029/2005GC001224.
Lodolo, E., Coren, F., Schreider, A.A., Ceccone, G., 1997. Geophysical evidence of a relict oceanic crust in the southwestern Scotia Sea. Mar. Geophys. Res. 19, 439–450.
Ludwig, K.R., 1999. IsoplotEx v. 2.6. Berkeley Geochronological Center Special Publication no. 1a.
Lyle, M., Gibbs, S., Moore, T.C., Rea, D.K., 2007. Late Oligocene initiation of the Antarctic Circumpolar Current: evidence from the South Pacific. Geology 35, 691–694.
Macellari, C.E., Barrio, C.A., Manassero, M.J., 1989. Upper Cretaceous to Paleocene depositional sequences and sandstone petrography of southwestern Patagonia (Argentina and Chile). J. South Am. Earth Sci. 2, 223–239.
Martinioni, D.R., Olivero, E.B., Palamarczuk, S., 1999. Estratigrafía y discordancias del Cretácico Superior–Paleoceno en la región central de Tierra del Fuego, in Nañez, C. (Ed.), Simposio Paleogeno de America del Sur, Alanes del Servicio Geológico Minero Argentino, 33. Buenos Aires, 7–16.
Miller, K.G., Wright, J.D., Fairbanks, R.G., 1991. Unlocking the ice house: Oligocene–Miocene oxygen isotopes, eustasy, and margin erosion. J. Geophys. Res. 96, 6829–6848.
Mukasa, S.B., Dalziel, I.W.D., 1996. Southernmost Andes and South Georgia Islands, North Scotia Ridge: zircon U–Pb and muscovite $^{40}Ar/^{39}Ar$ age constrains on tectonic evolution of southern Gondwanaland. J. South Am. Earth Sci. 9, 349–365.
Najman, Y., Carter, A., Oliver, G., Garzanti, E., 2005. Provenance of Eocene foreland basin sediments, Nepal: constraints to the timing and diachroneity of early Himalayan orogenesis. Geology 33, 309–312.
Nelson, E., 1982. Post-tectonic uplift of the Cordillera Darwin orogenic core complex, evidence from fission track geochronology and closing temperature–time relationships. J. Geol. Soc. Lond. 139, 755–761.
Olivero, E.B., 2002. Petrografia sedimentaria de sistemas turbiditicos del Cretacico–Paleogeno, Andes Fueguinos: prodencia, volcanismo y deformación. Actas Del XV Congreso Geologico Argentino, pp. 611–612.
Olivero, E.B., Malumián, N., 1999. Eocene stratigraphy of southeastern Tierra del Fuego, Argentina. Bull. Am. Assoc. Pet. Geol. 83, 295–313.
Olivero, E.B., Malumián, N., 2008. Mesozoic–Cenozoic stratigraphy of the Fuegian Andes, Argentina. Geosur: Mesozoic to Quaternary Evolution of Tierra del Fuego and Neighbouring Austral Regions II: Geologica Acta, vol. 6, pp. 5–18.
Olivero, E.B., Martinioni, D.R., 2001. A review of the geology of the Argentinian Fuegian Andes. J. South Am. Earth Sci. 14, 175–188.
Olivero, E.B., Malumián, N., Palamarczuk, S., 2003. Estratigrafía del Cretácico superior–Paleoceno del área de Bahía Thetis, Andes Fueguinos, Argentina: acontecimientos tectónicos y paleobiológicos. Rev. Geol. Chile 30, 245–263.
Olivero, E.B., Malumián, N., Palamarczuk, S., Scasso, R.A., 2002. El Cretácico superior–Paleógeno del área del Río Bueno, costa Atlántica de la Isla Grande de Tierra del Fuego. Rev. Asoc. Geol. Argent. 57, 199–218.
Pagani, M., Zachos, J.C., Freeman, K.H., Tripple, B., Bohaty, S., 2005. Marked decline in atmospheric carbon dioxide concentrations during the Paleogene. Science 390, 600–603.
Pankhurst, R.J., Leat, P.T., Sruoga, P., Rapela, C.W., Márquez, M., Storey, B.C., Riley, T.R., 1998. The Chon Aike silicic igneous province of Patagonia and related rocks in Antarctica: a silicic LIP. J. Volcanol. Geotherm. Res. 81, 113–136.
Pankhurst, R.J., Riley, T.R., Fanning, C.M., Kelley, S., 2000. Episodic silicic volcanism in Patagonia and the Antarctic Peninsula: chronology of magmatism associated with the break-up of Gondwana. J. Petrol. 41, 605–625.
Pfuhl, H.A., McCave, I.N., 2005. Evidence for late Oligocene establishment of the Antarctic Circumpolar Current. Earth Planet. Sci. Lett. 235, 715–728.
Rapalini, A.E., 2007. A paleomagnetic analysis of the Patagonian Orocline. Geol. Acta 5, 287–294.
Riley, T.R., Leat, P.T., 1999. Large volume silicic volcanism along the proto-Pacific margin of Gondwana: lithological and stratigraphical investigations from the Antarctic Peninsula. Geol. Mag. 136, 1–16.
Robinson, D.M., DeCelles, P.G., Patchett, P.J., Garzione, C.N., 2001. The kinematic evolution of the Nepalese Himalaya interpreted from Nd isotopes. Earth Planet. Sci. Lett. 192, 507–521.
Rolando, A., Hartmann, L.A., Santos, J.O.S., Fernandez, R.R., Etcheverry, R.O., Schalamuk, I.A., McNaughton, N.J., 2002. SHRIMP zircon U/Pb evidence for extended Mesozoic magmatism in the Patagonian batholith and assimilation Hubbard, S.M., Covault, J. of Archean crustal components. J. South Am. Earth Sci. 15, 267–283.
Romans, B.W., Fildani, A., Graham, S.A., Hubbard, S.M., Covault, J., in press. Importance of predecessor basin history on sedimentary fill of a retroarc foreland basin: Provenance analysis of the Cretaceous Magallanes basin, Chile (50°S–52°S). Basin Res.
Scher, H.D., Martin, E.E., 2006. Timing and climatic consequences of the opening of Drake Passage. Science 312, 428–430.
Stacey, J.S., Kramers, J.D., 1975. Approximation of terrestrial lead isotope evolution by a two-stage model. Earth Planet. Sci. Lett. 26, 207–221.
Stern, C.R., Mukasa, S.B., Fuenzalida, R., 1992. Age and petrogenesis of the Sarmiento ophiolite complex of southern Chile. J. South Am. Earth Sci. 6, 97–104.
Thomson, S.N., Herve, F., 2002. New time constraints for the age of metamorphism at the ancestral Pacific Gondwana margin of southern Chile (42–52°S). Rev. Geol. Chile 29, 255–271.
Torres Carbonell, P.J., Olivero, E.B., Dimieri, L.V., 2008. Structure and evolution of the Fuegian Andes foreland thrust-fold belt, Tierra del Fuego, Argentina: paleogeographic implications. J. South Am. Earth Sci. 25, 417–439.
Weislogel, A.L., Graham, S.A., Chang, E.Z., Wooden, J.L., Gehrels, G.E., Yang, H.S., 2006. Detrital zircon provenance of the Late Triassic Songpan–Ganzi complex: sedimentary record of collision of the North and South China blocks. Geology 34, 97–100.
Willan, R.C.R., Hunter, M.A., 2005. Basin evolution during the transition from continental rifting to subduction: evidence from the lithofacies and modal petrology of the Jurassic Latady Group, Antarctic Peninsula. J. South Am. Earth Sci. 20, 171–191.
Wilson, T.J., 1991. Transition from back-arc to foreland basin development in the southernmost Andes: stratigraphic record from the Ultima Esperanza District, Chile. Geol. Soc. Amer. Bull. 103, 98–111.
Winn, R.D., Dott Jr., R.H., 1979. Deep-water fan-channel conglomerates of Late Cretaceous age, southern Chile. Sedimentology 26, 203–228.
Zachos, J., Pagani, M., Sloan, L., Thomas, E., Billups, K., 2001. Trends, rhythms and aberrations in global climate, 65 Ma to present. Science 292, 686–693.